HHS Public Access

Author manuscript

ACS ES T Water. Author manuscript; available in PMC 2024 August 11.

Published in final edited form as:

ACS ES T Water. 2023 August 11; 3(8): 2009–2023. doi:10.1021/acsestwater.3c00111.

Recent Advances in the Removal of Radioactive Iodine and Iodide from the Environment

Siddappa A. Patil,
Department of Chemistry & Physics, Florida Gulf Coast University, Fort Myers, Florida 33965, United States; Centre for Nano and Material Sciences, Jain University, Kanakapura 562112, India

Raúl R. Rodríguez-Berríos,
Department of Chemistry, University of Puerto Rico, San Juan, Puerto Rico 00931-3346, United States

David Chavez-Flores,
Facultad de Ciencias Químicas, Universidad Autónoma de Chihuahua, Chihuahua 31125, México

Durgesh V. Wagle,
Department of Chemistry & Physics, Florida Gulf Coast University, Fort Myers, Florida 33965, United States

Alejandro Bugarin
Department of Chemistry & Physics, Florida Gulf Coast University, Fort Myers, Florida 33965, United States

Abstract

Iodine (I_2) in the form of iodide ions (I^-) is an essential chemical element in the human body. Iodine is a nonmetal that belongs to the VIIA group (halogens) in the periodic table. Over the last couple of centuries, the exponential growth of human society triggered by industrialization coincided with the use of iodine in a wide variety of applications, including chemical and biological processes. However, through these processes, the excess amount of iodine eventually ends up contaminating soil, underground water, and freshwater sources, which results in adverse effects. It enters the food chain and interferes with biological processes with serious physiological consequences in all living organisms, including humans. Existing removal techniques utilize different materials such as metal–organic frameworks, layered double hydroxides, ion-exchange resins, silver, polymers, bismuth, carbon, soil, MXenes, and magnetic-based materials. From our literature survey, it was clear that absorption techniques are the most frequently experimented

Corresponding Authors: **Alejandro Bugarin** – *Department of Chemistry & Physics, Florida Gulf Coast University, Fort Myers, Florida 33965, United States*; abugarin@fgcu.edu; **Durgesh V. Wagle** – *Department of Chemistry & Physics, Florida Gulf Coast University, Fort Myers, Florida 33965, United States*; dwagle@fgcu.edu; **Siddappa A. Patil** – *Department of Chemistry & Physics, Florida Gulf Coast University, Fort Myers, Florida 33965, United States; Centre for Nano and Material Sciences, Jain University, Kanakapura 562112, India*; p.siddappa@jainuniversity.ac.in.

Author Contributions

Alejandro Bugarin, Siddappa A. Patil, and Durgesh V. Wagle conceived, designed the paper structure, and collected most of the reviewed articles. The manuscript was written through equal contributions of all authors. All authors have given approval to the final version of the manuscript.

Complete contact information is available at: https://pubs.acs.org/10.1021/acsestwater.3c00111

The authors declare no competing financial interest.

with. In this Review, we have summarized current advancements in the removal of iodine and iodide from human-made contaminated aqueous waste.

Graphical Abstract

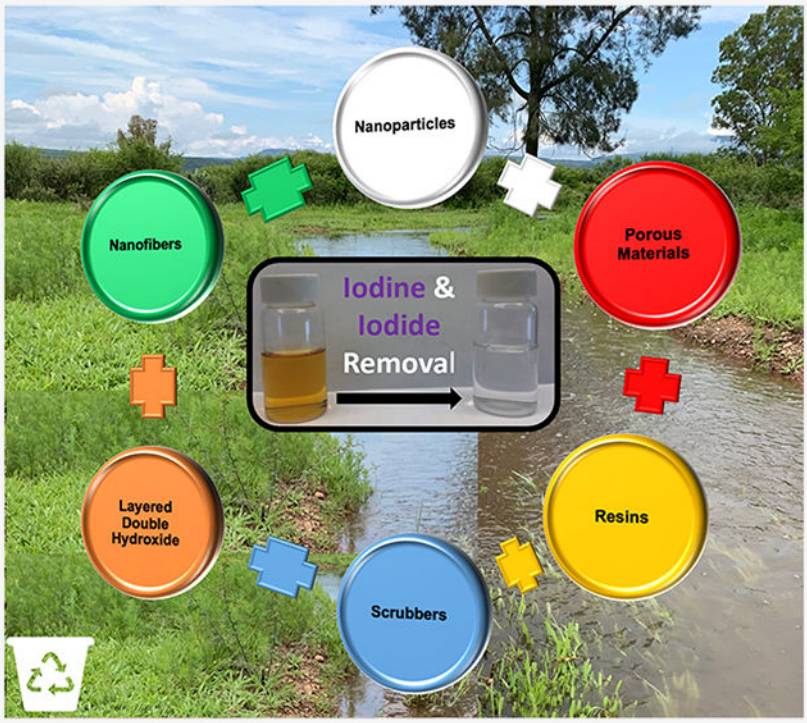

1. INTRODUCTION

Iodine is the 53rd element in the periodic table. However, the molecular form (I_2) is not found in nature, whereas *iodide* is the anion of iodine (I^-) that can pair with cations of metallic elements such as calcium, sodium, potassium, etc. to form salts that are commonly found in nature or can be produced synthetically. These iodide salts can be found in seaweed and mineral deposits, to name some potential sources of iodine.[1] Bernard Courtois discovered iodine in 1811 through a fortuitous accident during the period of the Napoleonic wars. At the time, the French army needed large amounts of potassium nitrate or saltpeter (KNO_3) for making gunpowder, which was sourced from the ashes of seaweed. During the process of making KNO_3, Courtois added an excess amount of sulfuric acid to the reaction mixture, which led to the formation of purple cloud-like vapors that later on condensed into lustrous crystals. Two years later in 1813, Joseph Gay-Lussac named these crystals iodine, a word derived from the Greek word *iodes*, meaning “violet-colored”.[1] Since then, applications of iodine have expanded beyond gunpowder manufacturing as a byproduct in the form of iodide salts that have found utility in a variety of applications such as photographic chemicals, disinfectants, inks, dyes, catalysts, feed supplements, polarizing filters for liquid crystal displays (LCDs), and radiotherapy, among many others (Figure 1). Although these miscellaneous uses are beneficial to our society,[2–4] they do produce large

quantities of iodine waste,[5–7] some even radioactive,[8] that spread around the globe, causing environmental disasters. Therefore, in a quest to mitigate these environmental effects, several research groups have put in significant efforts to tackle this issue by exploring different chemical/physical approaches through development of new materials to remove iodine from our environment.[9]

More specifically, the reported studies have focused on developing different strategies and materials for iodine removal, such as nanoparticles,[10] membrane filters (reverse osmosis,[11–14] nanofiltration,[11,13–17] ion exchange,[18,19] and electrodialysis[20]), electrochemical techniques,[21,22] absorption techniques (layered double hydroxides,[23–28] modified activated carbon,[27,29–31] silver impregnated activated carbon,[32,33] silver-doped carbon aerogels,[34–37] ion exchange resins,[38,39] soils,[40–42] and composites[43]), and oxidants.[44]

There are 37 known isotopes of iodine (^{108}I to ^{144}I), and all isotopes decay except ^{127}I, which is a stable isotope of iodine that is used in the applications listed below. In chemistry, ^{127}I is primarily used in oxidation reactions,[45] while in medicine, KI (^{127}I) is used as a supplement to protect against radioactive iodine. Radioactive isotopes of iodine, ^{123}I and ^{125}I, are used as nuclear imaging tracers to evaluate the physiological function of the thyroid glands, whereas, ^{131}I (half-life of 8 days) is used for the treatment of thyroid cancer or other physiological conditions of the thyroid glands (e.g., hyperthyroidism).[46] The use of this artificial radioisotope (^{131}I) has saved many lives, including my brother's (MVZ Alfredo Bugarin Cervantes). He was treated with radioactive ^{131}I for his thyroid condition (hyperthyroidism). Two weeks after his treatment, he drove through the United States–Mexico border, where nuclear radiation alarms sounded halfway into the Rio Grande bridge. His truck was stopped and surrounded by armed border patrol officers, and after interrogation, he was released. For us, it was an incredible experience to determine the sensitivity of those alarms that were able to detect such trace amounts of radioactive isotopes and secure our borders. The radioactive and stable isotopes of iodine are widespread in our environment, including soil and freshwater sources, and the production of iodine waste is inevitable, thus making it imperative to develop cost-effective and efficient technologies for the removal of iodine from the environment. Recently, Asmussen et al. documented developments of iodine wasteform production.[47] They described current efforts to develop materials capable of the capture, recovery conversion, and disposal of iodine. They also mentioned the highly toxic radioiodine, which is an inevitable waste byproduct from nuclear fission released during standard operation of nuclear power plants or by accidents such as the Fukushima and Chernobyl disasters.[48] Besides people working in nuclear power plants that might be exposed to radioiodine emission, iodine ions can also come from other sources such as chemical plants, pharmaceutical industries, food processing, high-tech industries, and hospitals. Wastewater polluted with iodine causes contamination of potable and groundwater,[49] which will increase the risk of thyroid cancer.[50] Typically, exposure to iodine could present short-term effects such as (1) irritation, skin burns, and eyes damage; (2) fumes that might harshly irritate both nose and throat; and (3) headache, metallic taste, nausea, vomiting, diarrhea, and abdominal pain. Longer exposure or higher doses will cause chronic health effects including cancers and reproductive hazards, among others.[50]

In this review, we have organized and summarized the most up-to-date technologies and strategies developed for the removal of iodine from the environment and their potential extrapolation to the removal of radioactive iodine isotopes.

2. REMOVAL OF RADIOACTIVE IODINE

2.1. Metal–Organic Framework-Based Materials.

In recent times, the porous metal–organic framework (MOF) has emerged as a promising class of materials for the extraction of I_2 from gases and liquids. Xu et al. used {[Zn_3(DL-lac)$_2$(pybz)$_2$]·2.5DMF}n (lac-Zn), a porous zinc-based polycrystalline, double-walled MOF, for removal of radioactive I_2 from cyclohexane. In these MOFs, the presence of confined nanochannels that are lined with a π-electron wall and high pore volume resulted in maximum adsorption of I_2 of about 755 mg/g with an initial efficiency of 92.98%. Interestingly, this efficiency fell down to 78.21% within 216 min of adsorption. Mechanistic insight involving Raman characterization revealed the formation of I_3^- during the iodine capture.[51] A recyclable cross-linked chitosan-MOF composite (Figure 2a) demonstrated an I_2 removal capacity of 399.68 mg/g at room temperature from wastewater. This chitosan MOF demonstrated high chemical and thermal stability with better performance under acidic conditions. The mechanism indicated that chitosan allowed for increased I_2 adsorption through charge–charge ($–NH_3^+ \ldots I^-$) interactions between sugar and I_2. The authors also proposed an alternative mechanism in which the iodine adsorption happens through the formation of host–guest complexes.[52] A nanocomposite material, poly(vinylidene fluoride) (PVDF)/zeolite-based MOF (ZIF-8), was able to reach a maximum adsorption capacity of 73.33 mg/g with an I_2 removal efficiency of 73% after 180 min (Figure 2b). This composite material was pH-sensitive with a working range of pH 5 to 12 and maintained high I_2 removal efficiency for up to 5 cycles.[53] On the other hand, nanoflakes of multilayered zeolitic imidazolate frameworks-L (ZIF-L) deposited on a microporous silicon carbide membrane exhibited 100% and 96% removal efficiency for I_2 from cyclohexane. The high efficiency of ZIF-L was attributed to its hierarchical structure and 6-membered windows in the cagelike structure (Figure 2c).[54] A hybrid material of Cu_2O nanoparticles encapsulated with MOF-TMU-17-NH_2 exhibited an I_2 adsorption of 567 mg/g after 22 h at room temperature in liquid and vapor phases. The I_2 removal occurred through chemisorption, and the composite material exhibited 98% recyclability after 4 cycles.[55] A PVDF composite material containing 70 wt % zirconium-based MOF was synthesized by a phase inversion method and displayed a maximum I_2 adsorption capacity of 1.42 g/g at 80 °C, which increased at 120 °C. This MOF had a high readsorption capacity of up to 0.99 g/g in the third cycle.[56] A low-cost, dense, porous, natural basswood structure doped with zeolitic imidazolate MOF (ZIF-8) demonstrated I_2 adsorption capacities of 1.07 and 1.09 g/g from cyclohexane and N_2 stream, respectively. The porous vertical channel-like structure of the wood provided ideal conditions for the circulation of gas and solvent containing I_2. Although the ZIF-8/wood composite was 30 min slower to attain adsorption equilibrium compared to ZIF-8 alone, it displayed significantly better adsorption capacity and kinetics.[57] A 3D MOF ({[Mn_2(oxdz)$_2$(tpbn)(H_2O)$_2$]· 2C_2H_5OH}$_n$) containing flexible and angular carboxylic acid-based dual linkers and a flexible bis(tridentate) ligand displayed 100% reversible sorption of I_2 with an uptake capacity of 1100 ± 50 mg/g. The high adsorption

capacity is attributed to the large pore volume and interaction of I_2 with the π-system of the polarized oxadiazole moiety in the MOF. Mechanistic insights through simulations revealed that the incoming iodine interacted with the highly polarized electron-rich π-system of the oxadiazole moieties of the MOF.[58] Zhang et al. reported an open metal-sulfide-based MOF ($(NH_4)_2(Sn_3S_7)$) with I_2 sorption capacities of 2.12 and 6.12 g/g under dynamic and static conditions, respectively. A detailed mechanistic insight revealed that the MOF captured I_2 through chemical as well as physical adsorption of I_2. The porous framework of the MOF allowed for molecular diffusion that resulted in physical adsorption and a soft–soft interaction between S^{2-} and I_2. This led to the formation of S_8 and I^-. Furthermore, the NH_4^+ in the channels physically adsorbed I_3^- through electrostatic and hydrogen bonding interaction. As the adsorption progressed, Sn^{4+} reacted with I^- to form SnI_4, leading to unprecedented adsorption capacity of the MOF.[59] Wang et al. synthesized a thermally stable, highly porous, 3D covalent organic framework (COF) with inherent diamond topology knotted by adamantane units for I_2 capture. This COF with an 8-fold interwoven skeleton and 1D nanochannels lined with π-conjugated pore walls achieved exceptional I_2 sorption capacity of 2300 mg/g with an uptake capacity of 66 wt % under harsh conditions.[60] Interestingly, the adsorption and desorption cycles of I_2 caused structural changes in the COF that allowed for a high recyclability of up to 80% of the original capacity. Song et al. successfully tested an imine-based COF for I_2 extraction with high I_2 sorption capacities of up to 5.82 and 0.99 g/g in vapor and solution phases, respectively. It was interesting to find out that in addition to the high pore volume of this COF, the imine and the benzene moieties in the pore walls acted as binding sites for I_3^-.[61] A 3D mesoporous coordination polymer ($Ni_3(BTC)_2{\cdot}12H_2O$) was synthesized by using ultrasound irradiation to remove I_2 from a gas stream. The ultrasound irradiation and sequential dipping steps in the synthesis process allowed for well-directed growth of porous organic polymer (POP)[62] particles leading to controlled adsorption and desorption of I_2.[63]

2.2. Silver-Based Adsorbents.

A column covered with silver foil (Goodfellow, 0.020 ± 0.003 mm, purity = 99.9%) on the inner surface was used to adsorb radioactive I_2 that was produced by a MYRRHA reactor, a lead–bismuth eutectic cooled proton accelerator driven system. The silver material effectively adsorbed I_2 evaporated from the eutectic mixture at all tested conditions.[64] A silver-functionalized silica aerogel (AgAero) was tested for the safe sequestration of radioactive iodine from nuclear waste streams and subsurface environments. The AgAero exhibited selective, rapid, and complete removal of I_2 from deionized water, which was better than Hanford Site Waste Treatment Plant samples containing 5 to 10 ppm of I_2. The AgAero was able to remove all halides but preferentially removed I_2 over Br_2 and Cl_2.[65] The silver-exchange mordenite materials were studied for their I_2 adsorption, regeneration, and recycling abilities. The X-ray fluorescence data confirmed the formation of AgI within the mordenite channels in addition to surface AgI nanoparticles following I_2 exposure.[66] A silver-doped apatite $Pb_{10}(VO_4)_6I_2$ was evaluated for the removal of radioactive I_2 from waste streams. The I_2 uptake of the silver apatite was 9.0 wt % with a loading efficiency of 94.62%.[67] Kim et al. used Ag-coated spherical alumina particles for I_2 extraction from alkaline solutions. This composite material was very robust with I_2 removal and recovery efficiencies of 99.7% and 62%, respectively.[68]

2.3. Porous Organic Polymer-Based Materials.

Porous organic polymers (POPs) have emerged as a promising avenue for the extraction of I_2 from gaseous and liquid phases. Pan et al. developed a nitrogen- and sulfur-rich POP via a catalyst-free hydrothermal process that displayed an excellent reversible I_2 uptake capacity of 326 wt % for volatile I_2 at 78 °C and ambient temperature. Interestingly, this POP was able to release 78.3% of the adsorbed I_2 in methanol through a controlled release process. The POP displayed excellent recyclability (5 cycles), which was attributed to its high physicochemical stability.[69] Changani et al. reported a highly recyclable polydopamine/polypropylene membrane for I_2 extraction. The material was tested in static and dynamic conditions with extraction capacities of 245 and 206 mg/g, respectively. The study revealed the formation of I_3^- during the process, which interacted with the phenolic group of the dopamine and resulted in extraction of I_2 from the liquid phase (Figure 3).[70]

A pillar[5]arene-based microporous polymer with high nitrogen content had I_2 removal efficiencies of 222.5 wt % and 80% in solvent and vapor phases, respectively. The adsorption mechanism revealed the formation of I_3^- and I_5^- during the process, and I_2 uptake and sorption remained constant for up to 5 cycles.[71] Yu et al. synthesized a series of bisindole[3]arene (BID[3]) macrocycles with high iodine capture capacity ranging between 4.49 and 5.12 g/g. It was noted that these BID[3]s adsorbed 2.41 to 2.81 iodine molecules per indole unit, thus indicating that the iodine was adsorbed on the interior and exterior surfaces of the macrocycle. The FTIR analysis indicated disappearance/weakening of the C–N stretch upon iodine uptake, thus indicating the crucial role of indole in iodine capture.[72] A hyper-cross-linked, nitrogen-rich triazine- and pyrrole-based POP developed by Li et al., with a nitrogen content of 8.04 wt % and a surface area of 222.8 m^2/g, demonstrated an I_2 uptake capacity of 257 wt %. The high performance of this POP is attributed to the presence of an extended π-electron environment within the structure.[73]

2.4. Carbon-Based Materials.

A hollow carbon-based supported polyhedron nanoparticle adsorbent material synthesized by a wet impregnation method demonstrated an I_2 removal capacity of 40 mg/g. This material performed best at 10% carbon loading at 20 °C.[74] A commercially available activated carbon (KAD coal) with an average grain size of 2.25 mm had an I_2 adsorption capacity of 1.03 g/g for an I_2 solution with a concentration of 1 g/L. This material was robust, easy to recycle, and maintained high sorption capacity for up to 8 cycles.[75] Yilmaz et al. used a single-walled carbon nanotube (SWNT) which performed I_2 removal with an efficiency of 22.60% and an adsorption capacity of 1.356 mg/g. This performance was attributed to the large surface area and high adhesive strength of the SWNT after interaction with ^{131}I.[76] The removal percentage for ^{131}I follows the following order: SWNT (22.60%) > graphene oxide (18.01%) > –COOH-functionalized SWNT (15.28%) > graphene (14.63%) (Table 1).

2.5. Bismuth-Based Adsorbents.

Alsalbokh et al. investigated the extraction of I_2 from aqueous solutions using aminosilane-grafted mesoporous alumina (γ-Al_2O_3) in which they employed three types of aminosilanes.[77] But the mesoporous alumina containing 3-(*N,N*-

dimethylaminopropyl)trimethoxysilane (Al-DMAPS) showed the highest performance at 50 °C after 24 h with a 95% I_2 removal efficiency and an adsorption capacity of 241 mg/g (Table 2). The Al-DMAPS had 2.3–10.3% leaching of I_2 during the first 12 h and 30.4% after 24 h, indicating that this material is ideal for quick removal of I_2. Alsalbokh et al. investigated a series of aminosilane-grafted bismuth alumina (Bi_x/Al_2O_3) adsorbents for I_2 adsorption.[78] The study revealed the dependency of I_2 adsorption on the type and amount of amine used in the process, with Bi_{15}/Al-DMAPS exhibiting adsorption capacities of 215.7 mg/g (30 wt % DMAPS) and 251.5 mg/g (60 wt % DMAPS). The Bi_{15}/Al-DMAPS exhibited no signs of leaching even after 24 h, while Bi_{15}/Al_2O_3 leached 11% of I_2 after 8 h. Yang et al. developed bismuth-based poly(vinyl alcohol) (PVA) adsorbents with an I_2 removal capacity of 468 mg/g from off-gas stream.[79] This capacity is 1.9-fold higher than that of the commercial silver-exchanged zeolite (AgX). Their follow-up work on bismuth-embedded SBA-15 mesopores silica functionalized with thiol groups (Bi-SBA-15-SH) effectively captured I_2 with the highest capacity of 540 mg/g.[80] The leaching test revealed a nominal loss of 0.29% I_2, indicating long-term storage and disposal capabilities of Bi-SBA-15-SH. Bismuth-mordenite (Bi_x@ modernite) developed by Al-Mamoori and co-workers demonstrated an adsorption capacity of 538 mg/g for I_2 with a 2.5-fold enhancement relative to the bare zeolite and significantly better than Ag@modernite under harsh conditions.[81] Leaching studies revealed that at 25 °C, approximately 36% of the I_2 was released after 24 h, indicating a limitation as far as permanent geological disposal of I_2 is concerned.

2.6. MXene-Based Materials.

The 2D-layered MXene-PDA-Ag_2Ox hybrid material synthesized by using a combination of mussel-inspired chemistry and the deposition of Ag_2O_x nanoparticles (Figure 4a) had an I_2 adsorption capacity of 80 mg/g with 80% efficiency at pH 5. This efficiency dropped by 50% after 5 cycles of adsorption and desorption. Moreover, the performance of the material also reduced by 50% in the presence of CO_3^{2-} and Cl^- due to anionic interference.[82] Sha et al. reported MXene-based bismuth oxide (MXene-PDA-Bi_6O_7) composites with an I_2 adsorption capacity of 64.65 mg/g.[83] This material functioned at pH 5 with no significant change in performance after 5 cycles of adsorption and desorption. A modified ionic-liquid-functionalized MXene synthesized by using a combination of mussel-inspired chemistry and Michael addition reaction had a high adsorption capacity of about 694.4 mg/g and a removal efficiency of 90% (Figure 4b).[84] The cyclic adsorption–desorption study indicated a loss in performance after each cycle. They also performed another study on I_2 adsorption using polyionic liquid (PIL)-functionalized MXene (MXene-PIL) absorbent.[85] The MXene-PIL made by a microwave-assisted, multicomponent *in situ* reaction between polyionic liquid (PIL) and MXene had an adsorption capacity of 170 mg/g.

2.7. Column-Based Materials.

Hakimi Sakuma et al. extracted ^{125}I from an aqueous solution of NaI by using a chemical and column-based method and monitored it by using ^{125}I γ-ray analysis.[86] The coagulation–flocculation and pH experiments in the chemical method that used alum and Praestol exhibited the highest decontamination factor (DF) value of 2 at a pH range of 5–6, whereas the use of ferric chloride and Praestol resulted in a DF value of 4.8 in a pH range of

6–7. The column method conducted using soil and kaolin clay materials had a DF value of 3.2, indicating that the chemical method using ferric chloride and Praestol is the best method to remove ^{125}I ions from acid systems. Decamp et al. used a silver-doped CL and XAD-4 resin mixed-bed column for the removal and retention of ^{131}I from radioactive waste.[87] It was found that 1 grade CL resin was ideal for the ^{131}I extraction with retention yields of up to 88 ± 5%. Nandanwar et al. reported carbon nanopolyhedrons supported on Engleharld Titanosilicate-10 (C@eTs-10) as a sorbent for I_2 and Kr from off-gas stream using a continuous flow adsorption column system.[88] The sorbent containing 10 wt % C@ETS-10 had maximum sorption capacities of sorbent for I_2 and Kr of 57.77 and 0.2933 mg/g at 20 °C, respectively, thus making it an ideal candidate for I_2 and Kr capture from an off-gas stream using a continuous flow adsorption column.

2.8. Magnetic-Based Materials.

Madrakian et al. extracted I_2 from water samples using silica-coated magnetic nanoparticles coated with imidazole pendants (im-SCMNPs) (Figure 5).[89] The im-SCMNPs exhibited 98% removal efficiency and an adsorption capacity of 140 mg/g at pH 7 with a max loading of only 50 mg of im-SCMNPs. Attallah et al. tested three derivatives of synthetic hematite: fibers (SH1), granular nanohematite (SH2), and nanoparticles (SH3) for the removal of ^{131}I from aqueous solutions.[90] It was found that the SH1 had the highest removal efficiency (90%) and an absorption capacity of 26.74 mg/g of iodine for systems under the following conditions: pH 1, V/m 0.1 L/g, for 30 min at 25 °C, and an initial concentration of 300 ppm.

2.9. Layered Double Hydroxides.

Although most of the reported approaches focus on the removal of I^- from gas streams, it is imperative to also give credit to layered double hydroxides (LDHs) as important sorbent materials.[91] In this regard, Fetter et al. used various sol–gel and precipitated hydrotalcites for the sorption of $^{131}I^-$ from aqueous solutions.[92] The materials were tested at two thermal treatments: dried at 343 K and calcinated at 500 K during 2 h. The sorption data for calcinated hydrotalcites showed better I^- affinity than that of the dried samples. This could be due to removal of considerable amounts of CO_3^{2-}, NO_3^-, and Cl^- ions upon calcination that left open anionic sites of I^- sorption. Curtius et al. used Mg-Al-Cl-LDH hydrotalcite adsorbent prepared by following the coprecipitation method developed by Weiss and Toth for I^- sorption.[93,94] They reported 50% adsorption capacity for I^- by Mg-Al-Cl-LDH in the following conditions: initial concentration of 4.25×10^{-5} mol/L in water, at 25 °C, and pH 8.5 after equilibrium that was achieved after 2 days. The addition of a 0.01 M $MgCl_2$ solution significantly reduced the I^- adsorption capacity to 30% and no sorption at 0.1 M $MgCl_2$ due to the competing anion effect from Cl^-. Kentjono et al. studied the utility of LDHs (Mg-Al(NO_3)LDH) for the extraction of boron and I_2 from wastewater at a polarizer manufacturing facility in Taiwan.[95] Although the Mg-Al(NO_3)LDH had a nominal I_2 uptake capacity of 10.1 mg/g, it was more effective for boron removal. Theiss et al. used $Zn_6Al_2(OH)_{16}(CO_3)\cdot 4H_2O$ (3:1 Zn/Al) LDH sorbent for the removal of $^{127}I_2$ and $^{127}I^-$ from water.[96] A gram of Zn/Al LDH extracted 99.5% of I_2 but removed only 36.8% of I^-. Thus, this indicates that Zn/Al LDH is more efficient for the removal of I_2. Overall, three portions of 3 g of Zn/Al LDH were needed to completely remove all species of iodine.

2.10. Ion-Exchange Resins.

Yu et al. used an in-house setup of anion-exchange resin (Figure 6) for the removal of I_2 from crude salt water (obtained from a chlor-alkali plant), which was used for caustic soda production.[97] The salt water used contained 1.7 mg/L of iodine. The adsorption rate for all iodine species in pure water was much higher than in salt water due to the lack of a competitive anion effect. The sequence of adsorption capacity in pure water was $I^- > I_3^- > I_2 > IO_3^-$, while in salt water it was $I_2 > I_3^- > I^- > IO_3^-$. The adsorption of I_3^-, I^-, and IO_3^- was based on the anion-exchange mechanism, whereas the I_2 adsorption involved reaction of I_2 with Cl^- to form ClI_2^-. The scale-up experiment was able to reduce the concentration of iodine to up to 0.2 mg/L after 20 days of uninterrupted, continuous operation. Its actual exchange capacity was determined to be 1.75 mmol/g.

2.11. Other Materials.

Chen and co-workers studied I_2 removal by ionic liquid (IL) 1-butyl-3-methylimidazolium acetate [BMIM][Ac] from cyclohexane (containing 0.2644 and 0.3840 g/L of I_2) and monitored it with 1D and 2D correlation UV–vis spectroscopy.[98] They quantified and discriminated between certain features of the IL involved in the extraction process such as the halogen bonds and the induced force interaction, resulting in I_2 sorption. It was noted that the halogen bonds contributed about 100–91% to I_2 sorption in the time range of 140–590 min, while the induced force contributed only 0–9% during the same time period, thus indicating that in [BMIM][Ac] the I_2 extraction primarily occurs through the halogen bonds. Another comprehensive study involving a series of ILs found that the halogen bond played a critical role in I_2 extraction.[99] Interestingly, this work revealed that cations were mere spectators in the process, whereas halogen containing ILs bound I_2 tightly, thus explaining their higher extraction efficiencies as a result of halogen bonding.

DeSilva et al. reported a simple method to enhance the p-type semiconducting properties of CuI by removal of an excess amount of I_2 while using thiocyanate (SCN) as a dopant.[100] The excess I_2 was removed by simple digestion of CuI in acetonitrile as free I_2 reacted with Cu to form CuI. Ali et al. tested a self-priming venturi scrubber for the I_2 removal efficiency under submerged and nonsubmerged conditions. The submerged conditions indicated the highest efficiency of 99.9 ± 0.1%, which was higher than the nonsubmerged conditions.[101] Later on, Gulhane et al. studied the I_2 removal efficiency in a self-priming venturi scrubber under submerged conditions using different pH solutions as a scrubbing liquid.[102] The maximum iodine removal efficiency of 66.62% was achieved in solutions at pH 10. Zhou et al. studied the performance of I^- vapor adsorption in a self-priming venturi scrubber and reported that the absorption efficiency increases remained around 99% by adjusting the flow rate of an aqueous solution.[103] Bal and collaborators designed, developed, and fabricated a laboratory-scale venturi scrubber for the removal of I_2 in a filtered containment venting system (Figure 7).[104] The I_2 removal experiments were conducted using KI solution and compared with water as a scrubbing liquid. The I_2 removal efficiency with normal water was 70.13%, while the use of KI solution increased it to 82.32%, due to the fact that I_2 reacted with KI to form a more water-soluble potassium triiodide (KI_3).

3. REMOVAL OF RADIOACTIVE IODIDE

Iodide contamination produced as a byproduct of nuclear fission poses a serious environmental concern to the health of current and future generations. This is primarily due to high mobility, long half-life ($t_{1/2}$) of 1.7×10^7 years, and high solubility of I^- in water as an anion, ^{129}I, can easily bioaccumulate and concentrate in the thyroid, resulting in cancers.[50] This makes it imperative to reduce the levels of iodine in the environment through environmental policies and advancements in technology. In the following section, we discuss several methods and techniques for removal of iodide from aqueous media. The performance of these methods in terms of amount (mg) of I^- or I_2 adsorbed per gram of material (adsorption capacity (mg/g)) and removal efficiency (%) has been highlighted in Table 3.

3.1. Carbon and Metal-Doped Materials.

In one of the very initial studies on I^- extraction, Yang and co-workers used a microporous activated carbon fiber (ACF) material with a surface area of 1660 m^2/g as an efficient sorbent material for the removal of I^- from water, acetic acid, methanol, and ethanol-based solutions. The ACF was effective under static and dynamic conditions with an extraction capacity of 350 mg/g and was easily regenerated by He flushing at 200 °C, thus promoting easy recycle and reuse.[107] A similar study by Rong et al. used a mesoporous, hierarchical Al_2O_3 carbon fiber for the removal of I^- from water with a 92.3% extraction efficiency (Figure 9a).[108] Meanwhile, Qian and co-workers used a porous carbon sphere (PCS) derived from the carbonization of poly(vinylidene chloride) with unique surface morphology and pore size (0.8–1.2 nm) for the removal of I^-. The ideal length-to-diameter ratio (L/D) of the pore structure in PCS allowed for an elevation in the linear velocity of the flow of acetic acid and an increase in acceleration, thus promoting diffusion of I^- into the inner structure of PCS.[109] Previously, Ikari et al. used natural organic material (NOM)-based activated carbon (AC) to reveal the influence of factors like chlorination and presence of Br^- on the residual concentration of I^- in water. Cl_2 allowed for the formation of HOI that reacted with NOM to form absorbable iodine, whereas the presence of Br^- resulted in the formation of HOBr, which converted HOI to water-soluble IO_3^- anion, thus impeding I^- extraction.[110] A hydrothermally synthesized, amine-doped carbon aerogel exhibited a maximum I^- adsorption capacity of 0.1079 g/g. This material had a consistent adsorption behavior at 318 K and functioned optimally at low pH.[111] A carbon-doped, silica-based aerogel displayed an excellent I^- adsorption capacity of 2.5 mmol/g at low pH (1.5). The material followed a Langmuir adsorption isotherm model, which is indicative of the adsorption of I^- in the form of a monolayer. The high capacity of this material was attributed to the continuous 3D porous morphology within the sheetlike structure.[112] Mushtaq et al. fabricated a hybrid nanocomposite membrane composed of gold nanoparticles and cellulose acetate membranes with an I^- removal efficiency of 99.88% in a continuous, aqueous, and single filtration process.[113] This material was highly recyclable, took less than a minute to remove I^-, and maintained high efficiency and selectivity in the presence of a high concentration of competitive anions (i.e., PO_4^-, Cl^-, and OH^-).

Sánchez-Polo and co-workers used silver-activated carbon aerogel for the removal of Br^- and I^- from drinking water. The carbonization and activation of the aerogel led to an increase in porosity and number of binding sites for Ag adsorption that enhanced the capacity for halide removal from water.[114] The Ag-Ag_2O-coated carbon sphere composite material synthesized by Yu et al. performed optimally at pH 2.1 with an adsorption capacity of 374.91 mg/g. This composite material exhibited high selectivity in the presence of competitive anions with an exception of CO_3^- and was easily regenerated by ozonolysis for use in the next cycle (Figure 8a).[115] The CuO_2/Cu-doped activated carbon synthesized by Zhang and co-workers displayed >90% removal efficiency within 90 min for the removal of I^- from wastewater in a two-stage adsorption process.[116] Han and co-workers synthesized bismuth-functionalized graphene oxide (Bi-GO) to remove I^- and IO_3^- from an aqueous system.[117] The Bi-GO exhibited superior kinetics and selectivity over a commercial silver-exchanged zeolite with removal efficiencies of ≥95% for I^- and IO_3^-.

3.2. Metal-Doped Polymeric Resins.

Nabipoor Hassankiadeh et al. tested Ag-doped cationic resins for methyl iodide extraction from acetic acid under varying temperature and flow rate conditions. The Ag content in the resin is linearly correlated to iodide extraction; the better performance of Ag/Amberlyst 15 is attributed to the higher surface area and pore volume in the resin.[118] The study on silica-based, quaternized poly(4-vinylpyridine) ion-exchange resin by Ye et al. indicated that the resin worked best with solutions at pH 6 with an I^- concentration of 0.1 mmol/L (Figure 9b).[119] Sarri et al. studied high and low molecular weight polyethylenimine-epichlorohydrin resins, which were tested for I^- extraction from aqueous systems. The high molecular weight resin exhibited adsorption capacities of up to 638.8 and 603.3 mg/g at pH 3 and 7, respectively, whereas the low molecular weight resin had capacities of 552.4 and 507.5 mg/g, respectively. The performances of these polymer resins decreased by 50% and 80% in the presence of Cl^- and SO_4^- anions, respectively.[120] Baimenov et al. developed hydrophilic, polymer-based, Ag-doped cryogels: coallylamine-methacrylic acid-DMAA-BisAAm (AAC) and coallylamine-2-acrylamido-2-methyl-1-propanesulfonic acid-DMAA-BisAAm (SAC). These cryogels acted as a scaffolding to house Ag-NPs with AAC and SAC exhibiting maximum loading capacities for I^- adsorption of 326 and 247 mg/g, respectively.[121]

3.3. Metal Nanoparticle-Based Materials.

Zia et al. used a Ag/Fe_3O_4 nanocomposite which displayed an adsorption capacity of 847 mg/g for I_2 removal from aqueous media. This material exhibited high I^- selectivity in the presence of competitive ions (Cl^-, Br^-, and PO_4^-), good recyclability, and a removal efficiency of approximately 94% after 7 cycles.[122] Rosenberg et al. reported the removal of ^{131}I from soil by chemical treatment in the presence and absence of I^- carrier, H_2O_2, and $AgNO_3$.[105] The quantification of the I^- removal was performed using gamma spectroscopic analysis, which showed that 45 ± 1% of I_2 was removed using $AgNO_3$ and carrier, although a lower performance of 17 ± 1% was achieved using H_2O_2 and HNO_3 reagents. Mu et al. used layered sodium niobate nanofibers with anchored Ag_2O nanocrystals (Ag_2O-SNF) to remove radioactive I^- and Sr^{2+}.[106] The presence of Ag_2O on the nanofiber resulted in the formation of AgI and led to a high adsorption capacity (296 mg/g) with the removal of more

than 97% of the I^- anions from aqueous solution. The material displayed high performance in basic condition but can be used in acidic and neutral conditions as well. Mao et al. conducted a comparative study between Ag-, Cu-, and AgCu-doped Cu_2O nanoparticles and found that AgCu-doped Cu_2O nanoparticles (NPs) displayed excellent selectivity for I^- and worked well under various harsh conditions such as pH, presence of competitive anions, and seawater.[123] Their subsequent work on Cu-doped Cu_2O nanoparticles indicated sensitivity toward the presence of a competitive anion and exhibited a linear relationship between the amount of Cu content in the NPs and the capacity to remove I^- from aqueous solution (Figure 9c).[124] Jang et al. showed that the modified magnetic NPs coated with cationic surfactants, hexadecyltrimethylammonium, exhibited an adsorbent capacity of 322.42 mg/g. These NPs exhibited a maximum efficiency of 93.81% for solutions at pH 3.9, a temperature of 43 °C, and an initial I^- concentration of 113.8 mg/L with over 80% selectivity in the presence of competitive anions.[125]

3.4. Metal-Doped Hierarchical and Layered Materials.

Synthetic Ag-zeolite nanocomposites showed an efficiency of 94.85% for I^- removal from aqueous solutions via the formation of stable AgI in the material. The competing anions had a negligible effect on the performance of Ag-zeolite with a maximum capacity for I^- of up to 20.44 mg/g.[126] A similar study on natural zeolite decorated with Ag_2O and Ag^0 nanoparticles demonstrated an I^- removal capacity of 132 mg/g through the formation of AgI (Figure 9d). The I^- removal was higher than expected based on the Ag content. Postadsorption characterization of this zeolite indicated the formation of negatively charged AgI colloids that accounted for removal of an excess amount of I^-. The study indicated complete removal of I^- by zeolite composites at the 100 min mark for solutions containing 200 ppm of I^-.[127] Zhao et al. synthesized a silver-doped, water-soluble metal–organic framework (MOF) MIL-101(Cr)-SO_3Ag by reacting $AgNO_3$ with MOF MIL-101(Cr)SO_3H for the removal of I^- from aqueous systems. The uniform formation of $–SO_3^-$ (from $–SO_3H$), which has a high affinity for Ag(I), led to uniform distribution of Ag in the MOF. The Ag–MOF had significantly smaller surface area and pore size compared to the undoped MOF, but it displayed higher I^- adsorption capacity (244.2 mg/g) compared to the undoped MOF (94.1 mg/g). This higher sorption is due to the formation of AgI, as evident from PXRD and zeta potential measurements.[128] Liu et al. reported flowerlike micro/nanostructure bismuth oxide $Bi_2O_{2.33}$ for the removal of I^-.[48] The mesoporous structure of $Bi_2O_{2.33}$ led to high adsorption values of 284.9 mg/g (I^-) and 228.8 mg/g (IO_3^-) with low leaching efficiencies of 2.3% (I^-) and 0.8% (IO_3^-), respectively. The material is highly selective for I^-, but the adsorption efficiency lowered to 60% in seawater due to competition from the CO_3^{2-} and Cl^- ions. Zhang et al. synthesized hierarchically porous bismuth oxide/layered double hydroxide (Bi_2O_3/LDH) composites by using a combination of a biological template method, *in situ* growth, and deposition techniques to study the I_2 removal from aqueous solutions.[129] The I^- absorption studies revealed that for a 30 mg dosage of Bi_2O_3/LDH composites, the I^- removal efficiency was 94%. Interestingly, I_2 absorption dropped to 15.13% and 20.49% in the presence of CO_3^{-2} and F^- ions, respectively.

Liang et al. used a Mg/Al (4:1)-based calcined layered double hydroxide (CLDH) to extract I^- from wastewater. It was noted that this CLDH displayed the highest uptake capacity of 96 mg/g for I^-, which was attributed to the large size of I^- that was suitable for a lower charge density of CLDH.[130] Ma et al. developed nanocomposites of Mg/Al layered double hydroxide (MgAl-LDH) intercalated with polysulfide (S_x^-) groups. The control experiment revealed that the reducing property of polysulfide helped the conversion of I_2 to I_3^- while simultaneously oxidizing to S_8 promoted the chemisorption of I_2. Furthermore, it was observed that the MgAl-LDH physically adsorbed I_2, leading to high adsorption capacity despite its low BET surface area. The material displayed adsorption capacities from 1.32 to 1.52 g/g and a maximum adsorption of 152 wt %.[131] A similar study of calcined core–shell Fe_3O_4@Mg/Al LDH indicated that a 4:1 Mg/Al ratio efficiently elutes I^- from aqueous solutions with a capacity of 105.04 mg/g. This improved capacity was attributed to the maximum spacing between the hydroxide layers. Furthermore, the LDH performed with >80% efficiency for up to 4 cycles.[132] Theiss et al. used Zn–Al (3:1) LDH for I_2/I^- removal. This LDH exhibited an efficiency of 36.8% for the removal of I^-. The regeneration of the LDH after the first cycle was difficult, indicating that this material has a potential for long-term storage of I^-,[133] although it is worth noting that the LDH efficiency for the removal of I_2 is about 99.5%. Zang et al. used Bi_2O_3-decorated mesoporous silica for I^- removal from aqueous solutions (Figure 8b). The high surface area of mesoporous Bi_2O_3 in the hexagonally packed silica channels allowed for removal of up to 2.87 mmol/g (229.6 mg/g) of I^-. The mesoporous Bi_2O_3-based silica was able to selectively remove I^- in the presence of NO_3^- and Cl^-.[134] Sha et al. used MXene-polydopamine (PDA)-Bi_6O_7-based nanocomposites that exhibited an I^- adsorption capacity of 64.65 mg/g at equilibrium. The nanocomposite displayed pH sensitivity with an optimal performance at pH 5. The recycle experiment data revealed a decrease in the adsorption efficiency (<20%) in the third and higher cycles.[135] Liu et al. used CuCl to precipitate I^- from aqueous solutions. The results indicated an optimal removal efficiency of 95.8% at a dosage of I^- between 5 and 40 mg/L and a reaction time of 15 min. The presence of HCO_3^- reduced the efficiency of I^- removal to 76.0%.[136]

As depicted in Figure 10, the most used materials for the removal of I_2/I^- ions have been LDHs, followed by carbon-based materials and MOFs. Unfortunately, it is somehow difficult to really assess the advantages/disadvantages of each category. This is mainly due to their differences in composition, durability, stability, recyclability, efficiency, adsorption capabilities, and of course standardization protocols.[47] However, LDHs and carbon-based materials are relatively easy to prepare. Although MOFs act as better I_2/I^- ion sensors, they are impractical for use in industrial-scale processes because they are usually prepared as powders. Furthermore, POPs have shown higher iodine capacities when compared with MOFs and other adsorbents.[62]

4. CONCLUSION AND OUTLOOK

The contamination of the water environment with toxic inorganic and organic contaminants is a serious issue across the globe. Hence, the purification of water resources is of critical importance to improving or reaching sustainable ecosystems. Furthermore, it is necessary to develop environmentally friendly and highly effective procedures for the removal of toxic

and hazardous chemicals from water bodies. For many years, toxic heavy metals and ions such as I_2/I^- have been discharged by various industrial activities into water bodies, which causes many health issues for living organisms. Hence, it is essential to control the iodine concentration in water and the environment. However, a complete picture of the iodine removal methods from the water environment has not been drawn yet. Therefore, the present Review discussed miscellaneous methods reported in the literature for the removal of I_2/I^- ions from water.

For the selection of the best method for I_2/I^- ion removal, we should consider many key factors, including operation cost, ion concentration, materials used and cost, environmental impact, pH, removal efficiency, and disposal of the used materials. The reviewed methods can be classified into three broad categories: adsorption, membranes, and electrochemical techniques. Those three broad methods utilize materials. For instance, different adsorbents have been used (e.g., silver-based, carbon-based, bismuth-based, MXene-based, polymers-based, magnetic-based, and MOFs). For membranes, the most used techniques are nano- and microfiltration, reverse osmosis, and electrodialysis), while electrolysis and deionization are the preferred electrochemical techniques. From all the techniques, adsorption is one of the most promising methods used for the removal of I_2/I^- ions due to its straightforward operation, high removal rate, low cost, and scalability. However, their reusability is still challenging. Another disadvantage of adsorption techniques is the low ion selectivity, whereas membrane techniques are more efficient in doing this, albeit at highest cost.

In summary, I_2/I^- ion removal by adsorption and membrane approaches are the most practical techniques reported in the literature as seen by the number of publications. However, there are still a few challenging questions/issues that need further research such as the following: (A) How can the methods be scaled up? (B) Is it possible to implement continuous flow approaches? (C) Could those methods work equally at low or high ions' concentration? (D) Can the mass-to-mass adsorption and rate versus material used be standardized? (E) Are those reported methods I_2/I^- ion-selective? (F) What about metal leakage? (G) Is material regeneration possible, especially for the membrane approaches? (H) An assessment of energy consumption and environmental impact for all processes (from material preparation to recovery and disposal) must be completed. Therefore, future technologies should focus on sustainable and eco-friendly materials that can be produced at low cost, while maintaining excellent adsorption/desorption cycles for easy regeneration. It is also imperative that further studies include actual wastewater rather than lab-made solutions when investigating iodine/iodide removal. Finally, we expect this Review will inspire the scientific community to design and develop other smart, sustainable, and functional materials for the removal of I_2/I^- ions from the environment.

ACKNOWLEDGMENTS

All authors are thankful to their respective institutions for supporting this work.

Funding

This review article was in part supported by the National Institute of General Medical Sciences of the National Institutes of Health (NIH) under Award no. 1R15GM141726-01.

REFERENCES

(1). Christe K; Schneider S Iodine Chemical Element. Britannica; https://www.britannica.com/science/iodine (accessed 06/14/2023).

(2). Bichsel Y; von Gunten U Oxidation of Iodide and Hypoiodous Acid in the Disinfection of Natural Waters. Environ. Sci. Technol 1999, 33 (22), 4040–4045.

(3). Trofe TW; Inman GW; Johnson JD Kinetics of Monochloramine Decomposition in the Presence of Bromide. Environ. Sci. Technol 1980, 14 (5), 544–549.

(4). Kumar K; Day RA; Margerum DW Atom-Transfer Redox Kinetics: General-Acid-Assisted Oxidation of Iodide by Chloramines and Hypochlorite. Inorg. Chem 1986, 25 (24), 4344–4350.

(5). Land M; Reichard EG; Crawford SM; Everett RR; Newhouse MW; Williams CF Ground-Water Quality of Coastal Aquifer Systems in the West Coast Basin, Los Angeles County, California, 1999–2002. US Geol. Surv. Sci. Investig. Rep 2004-5067 2004, 1–80.

(6). Moran JE; Oktay SD; Santschi PH Sources of Iodine and Iodine 129 in Rivers. Water Resour. Res 2002, 38 (8), 24-1–24-10.

(7). Duranceau SJ Determination of the Total Iodide Content in Desalinated Seawater Permeate. Desalination 2010, 261 (3), 251–254.

(8). Inoue H Radioactive Iodine and Chloride Transport across a Paper Membrane Bearing Trimethylhydroxypropylammonium Anion Exchange Groups. J. Membr. Sci 2003, 222 (1–2), 53–57.

(9). Watson K; Farré MJ; Knight N Strategies for the Removal of Halides from Drinking Water Sources, and Their Applicability in Disinfection by-Product Minimisation: A Critical Review. J. Environ. Manage 2012, 110, 276–298. [PubMed: 22810000]

(10). Jung E; Moon HJ; Park T-J; Bong KW; Yu T Facile Aqueous-Phase Synthesis of Magnetic Iron Oxide Nanoparticles to Enhance the Removal of Iodine from Water. Sci. Adv. Mater 2017, 9 (10), 1847–1853.

(11). Drewes JE; Xu P; Heil D; Wang G Multibeneficial Use of Produced Water Treatment through High Pressure Membrane Treatment and Capacitive Deionization Technology. Reclam. Manage. Water West, 2009. https://www.usbr.gov/research/dwpr/reportpdfs/report133.pdf (accessed 06/14/2023).

(12). Duranceau SJ Determination of the Total Iodide Content in Desalinated Seawater Permeate. Desalination 2010, 261 (3), 251–254.

(13). Pontié M; Diawara CK; Rumeau M Streaming Effect of Single Electrolyte Mass Transfer in Nanofiltration: Potential Application for the Selective Defluorination of Brackish Drinking Waters. Desalination 2003, 151 (3), 267–274.

(14). Pontie M; Buisson H; Diawara CK; Essis-Tome H Studies of Halide Ions Mass Transfer in Nanofiltration – Application to Selective Defluorination of Brackish Drinking Water. Desalination 2003, 157 (1–3), 127–134.

(15). Harrison CJ; Le Gouellec YA; Cheng RC; Childress AE Bench-Scale Testing of Nanofiltration for Seawater Desalination. J. Environ. Eng 2007, 133 (11), 1004–1014.

(16). Diawara CK; Lô SM; Rumeau M; Pontie M; Sarr O A Phenomenological Mass Transfer Approach in Nanofiltration of Halide Ions for a Selective Defluorination of Brackish Drinking Water. J. Membr. Sci 2003, 219 (1–2), 103–112.

(17). Lhassani A Selective Demineralization of Water by Nanofiltration Application to the Defluorination of Brackish Water. Water Res. 2001, 35 (13), 3260–3264. [PubMed: 11487124]

(18). Weiss J; Jensen D Modern Stationary Phases for Ion Chromatography. Anal. Bioanal. Chem 2003, 375 (1), 81–98. [PubMed: 12520442]

(19). Nightingale ER Phenomenological Theory of Ion Solvation. Effective Radii of Hydrated Ions. J. Phys. Chem 1959, 63 (9), 1381–1387.

(20). Inoue H; Kagoshima M Removal of 125I from Radioactive Experimental Waste with an Anion Exchange Paper Membrane. Appl. Radiat. Isot 2000, 52 (6), 1407–1412. [PubMed: 10855669]

(21). Xu P; Drewes JE; Heil D; Wang G Treatment of Brackish Produced Water Using Carbon Aerogel-Based Capacitive Deionization Technology. Water Res. 2008, 42 (10–11), 2605–2617. [PubMed: 18258278]

(22). Ying T-Y; Yang K-L; Yiacoumi S; Tsouris C Electrosorption of Ions from Aqueous Solutions by Nanostructured Carbon Aerogel. J. Colloid Interface Sci 2002, 250 (1), 18–27. [PubMed: 16290630]

(23). Thomas N; Rajamathi M Intracrystalline Oxidation of Thiosulfate-Intercalated Layered Double Hydroxides. Langmuir 2009, 25 (4), 2212–2216. [PubMed: 19170507]

(24). Theiss FL; Ayoko GA; Frost RL Iodide Removal Using LDH Technology. Chem. Eng. J 2016, 296, 300–309.

(25). Pless JD; Benjamin Chwirka J; Krumhansl JL Iodine Sequestration Using Delafossites and Layered Hydroxides. Environ. Chem. Lett 2007, 5 (2), 85–89.

(26). Liang L; Li L Adsorption Behavior of Calcined Layered Double Hydroxides towards Removal of Iodide Contaminants. J. Radioanal. Nucl. Chem 2007, 273 (1), 221–226.

(27). Kaufhold S; Pohlmann-Lortz M; Dohrmann R; Nüesch R About the Possible Upgrade of Bentonite with Respect to Iodide Retention Capacity. Appl. Clay Sci 2007, 35 (1–2), 39–46.

(28). Kentjono L; Liu JC; Chang WC; Irawan C Removal of Boron and Iodine from Optoelectronic Wastewater Using Mg–Al (NO_3) Layered Double Hydroxide. Desalination 2010, 262 (1–3), 280–283.

(29). Mianowski A; Owczarek M; Marecka A Surface Area of Activated Carbon Determined by the Iodine Adsorption Number. Energy Sources Part Recovery Util. Environ. Eff 2007, 29 (9), 839–850.

(30). Zhang X; Gu P; Li X; Zhang G Efficient Adsorption of Radioactive Iodide Ion from Simulated Wastewater by Nano Cu_2O/Cu Modified Activated Carbon. Chem. Eng. J 2017, 322, 129–139.

(31). Balsley SD; Brady PV; Krumhansl JL; Anderson HL Anion Scavengers for Low-Level Radioactive Waste Repository Backfills. J. Soil Contam 1998, 7 (2), 125–141.

(32). Hoskins JS; Karanfil T; Serkiz SM Removal and Sequestration of Iodide Using Silver-Impregnated Activated Carbon. Environ. Sci. Technol 2002, 36 (4), 784–789. [PubMed: 11878398]

(33). Ho PC; Kraus KA Adsorption on Inorganic Materials—VIII: Adsorption of Iodide on AgCl-Filled Carbon. J. Inorg. Nucl. Chem 1981, 43 (3), 583–587.

(34). Sánchez-Polo M; Rivera-Utrilla J; von Gunten U Bromide and Iodide Removal from Waters under Dynamic Conditions by Ag-Doped Aerogels. J. Colloid Interface Sci 2007, 306 (1), 183–186. [PubMed: 17109877]

(35). Sánchez-Polo M; Rivera-Utrilla J; Salhi E; von Gunten U Removal of Bromide and Iodide Anions from Drinking Water by Silver-Activated Carbon Aerogels. J. Colloid Interface Sci 2006, 300 (1), 437–441. [PubMed: 16696995]

(36). Sánchez-Polo M; Rivera-Utrilla J; von Gunten U Metal-Doped Carbon Aerogels as Catalysts during Ozonation Processes in Aqueous Solutions. Water Res. 2006, 40 (18), 3375–3384. [PubMed: 16970972]

(37). Sánchez-Polo M; Rivera-Utrilla J; Salhi E; von Gunten U Ag-Doped Carbon Aerogels for Removing Halide Ions in Water Treatment. Water Res. 2007, 41 (5), 1031–1037. [PubMed: 16970974]

(38). Lokhande RS; Singare PU; Patil AB A Study of Ion Exchange Equilibrium for Some Uni-Univalent and Uni-Divalent Reaction Systems Using Strongly Basic Anion Exchange Resin Indion-830 (Type 1). Russ. J. Phys. Chem. A 2007, 81 (12), 2059–2063.

(39). Lokhande RS; Singare PU; Parab SA Application of Radioactive Tracer Technique to Study the Kinetics of Iodide Ion-Isotope Exchange with Strongly Basic Anion-Exchange Resin Duolite A-116. Radiochemistry 2008, 50 (6), 642–644.

(40). Yoshida S; Muramatsu Y; Uchida S Studies on the Sorption of I- (Iodide) and IO3- (Iodate) onto Andosols. Water. Air. Soil Pollut 1992, 63 (3–4), 321–329.

(41). Dai JL; Zhang M; Hu QH; Huang YZ; Wang RQ; Zhu YG Adsorption and Desorption of Iodine by Various Chinese Soils: II. Iodide and Iodate. Geoderma 2009, 153 (1–2), 130–135.

(42). Muramatsu Y; Uchida S; Sriyotha P; Sriyotha K Some Considerations on the Sorption and Desorption Phenomena of Iodide and Iodate on Soil. Water. Air. Soil Pollut 1990, 49 (1–2), 125–138.

(43). Liu S; Wang N; Zhang Y; Li Y; Han Z; Na P Efficient Removal of Radioactive Iodide Ions from Water by Three-Dimensional Ag2O–Ag/TiO2 Composites under Visible Light Irradiation. J. Hazard. Mater 2015, 284, 171–181. [PubMed: 25463231]

(44). Huang KZ; Zhang H Highly Efficient Bromide Removal from Shale Gas Produced Water by Unactivated Peroxymonosulfate for Controlling Disinfection Byproduct Formation in Impacted Water Supplies. Environ. Sci. Technol 2020, 54 (8), 5186–5196. [PubMed: 32202106]

(45). Dess DB; Martin JC Readily Accessible 12-I-5 Oxidant for the Conversion of Primary and Secondary Alcohols to Aldehydes and Ketones. J. Org. Chem 1983, 48 (22), 4155–4156.

(46). Robison LM; Sylvester PW; Birkenfeld P; Lang JP; Bul RJ Comparison of the Effects of Iodine and Iodide on Thyroid Function in Humans. J. Toxicol. Environ. Health A 1998, 55 (2), 93–106. [PubMed: 9761130]

(47). Asmussen RM; Turner J; Chong S; Riley BJ Review of Recent Developments in Iodine Wasteform Production. Front. Chem 2022, 10, 1043653. [PubMed: 36618856]

(48). Liu S; Kang S; Wang H; Wang G; Zhao H; Cai W Nanosheets-Built Flowerlike Micro/Nanostructured Bi2O2.33 and Its Highly Efficient Iodine Removal Performances. Chem. Eng. J 2016, 289, 219–230.

(49). Han W; Clarke W; Pratt S Cycling of Iodine by Microalgae: Iodine Uptake and Release by a Microalgae Biofilm in a Groundwater Holding Pond. Ecol. Eng 2016, 94, 286–294.

(50). Balter M Chernobyl's Thyroid Cancer Toll. Science 1995, 270 (5243), 1758–1759. [PubMed: 8525362]

(51). Xu L; Zheng Q; Wang Y; Jiang L; Jiang J; Qiu J A Pillared Double-Wall Metal-Organic Framework Adsorption Membrane for the Efficient Removal of Iodine from Solution. Sep. Purif. Technol 2021, 274, 118436.

(52). El-Shahat M; Abdelhamid AE; Abdelhameed RM Capture of Iodide from Wastewater by Effective Adsorptive Membrane Synthesized from MIL-125-NH2 and Cross-Linked Chitosan. Carbohydr. Polym 2020, 231, 115742. [PubMed: 31888810]

(53). Long X; Chen Y-S; Zheng Q; Xie X-X; Tang H; Jiang L-P; Jiang J-T; Qiu J-H Removal of Iodine from Aqueous Solution by PVDF/ZIF-8 Nanocomposite Membranes. Sep. Purif. Technol 2020, 238, 116488.

(54). Xiao H; Zhou H; Feng S; Gore DB; Zhong Z; Xing W In Situ Growth of Two-Dimensional ZIF-L Nanoflakes on Ceramic Membrane for Efficient Removal of Iodine. J. Membr. Sci 2021, 619, 118782.

(55). Yadollahi M; Hamadi H; Nobakht V Capture of Iodine in Solution and Vapor Phases by Newly Synthesized and Characterized Encapsulated Cu2O Nanoparticles into the TMU-17-NH2MOF. J. Hazard. Mater 2020, 399, 122872. [PubMed: 32521316]

(56). Wang L; Chen P; Dong X; Zhang W; Zhao S; Xiao S; Ouyang Y Porous MOF-808@ PVDF Beads for Removal of Iodine from Gas Streams. RSC Adv. 2020, 10 (73), 44679–44687. [PubMed: 35516247]

(57). Wang Z; He Y; Zhu L; Zhang L; Liu B; Zhang Y; Duan T Natural Porous Wood Decorated with ZIF-8 for High Efficient Iodine Capture. Mater. Chem. Phys 2021, 258, 123964.

(58). Gogia A; Das P; Mandal SK Tunable Strategies Involving Flexibility and Angularity of Dual Linkers for a 3D Metal–Organic Framework Capable of Multimedia Iodine Capture. ACS Appl. Mater. Interfaces 2020, 12 (41), 46107–46118. [PubMed: 32957781]

(59). Zhang Y; He L; Pan T; Xie J; Wu F; Dong X; Wang X; Chen L; Gong S; Liu W; Kang L; Chen J; Chen L; Chen L; Han Y; Wang S Superior Iodine Uptake Capacity Enabled by an Open Metal-Sulfide Framework Composed of Three Types of Active Sites. CCS Chem. 2023, 5 (7), 1540–1548.

(60). Wang C; Wang Y; Ge R; Song X; Xing X; Jiang Q; Lu H; Hao C; Guo X; Gao Y; et al. A 3D Covalent Organic Framework with Exceptionally High Iodine Capture Capability. Chem. Eur. J 2018, 24 (3), 585–589. [PubMed: 29178592]

(61). Song S; Shi Y; Liu N; Liu F C═N Linked Covalent Organic Framework for the Efficient Adsorption of Iodine in Vapor and Solution. RSC Adv. 2021, 11 (18), 10512–10523. [PubMed: 35423582]

(62). Zhang X; Maddock J; Nenoff TM; Denecke MA; Yang S; Schröder M Adsorption of Iodine in Metal–Organic Framework Materials. Chem. Soc. Rev 2022, 51 (8), 3243–3262. [PubMed: 35363235]

(63). Azadbakht A; Abbasi AR; Noori N Layer-by-Layer Synthesis of Nanostructure NiBTC Porous Coordination Polymer for Iodine Removal from Wastewater. J. Inorg. Organomet. Polym. Mater 2016, 26 (2), 479–487.

(64). Karlsson E; Neuhausen J; Eichler R; Danilov II; Vögele A; Türler A Silver as a Capturing Material for Iodine Released from Lead–Bismuth Eutectic in Various Conditions. J. Radioanal. Nucl. Chem 2021, 328 (2), 707–715.

(65). Asmussen RM; Matyáš J; Qafoku NP; Kruger AA Silver-Functionalized Silica Aerogels and Their Application in the Removal of Iodine from Aqueous Environments. J. Hazard. Mater 2019, 379, 119364. [PubMed: 29753522]

(66). Abney CW; Nan Y; Tavlarides LL X-Ray Absorption Spectroscopy Investigation of Iodine Capture by Silver-Exchanged Mordenite. Ind. Eng. Chem. Res 2017, 56 (16), 4837–4846.

(67). Cao C; Chong S; Thirion L; Mauro JC; McCloy JS; Goel A Wet Chemical Synthesis of Apatite-Based Waste Forms–A Novel Room Temperature Method for the Immobilization of Radioactive Iodine. J. Mater. Chem. A 2017, 5 (27), 14331–14342.

(68). Kim T; Lee S-K; Lee S; Lee JS; Kim SW Development of Silver Nanoparticle–Doped Adsorbents for the Separation and Recovery of Radioactive Iodine from Alkaline Solutions. Appl. Radiat. Isot 2017, 129, 215–221. [PubMed: 28923588]

(69). Pan X; Ding C; Zhang Z; Ke H; Cheng G Functional Porous Organic Polymer with High S and N for Reversible Iodine Capture. Microporous Mesoporous Mater. 2020, 300, 110161.

(70). Changani Z; Razmjou A; Taheri-Kafrani A; Warkiani ME; Asadnia M Surface Modification of Polypropylene Membrane for the Removal of Iodine Using Polydopamine Chemistry. Chemosphere 2020, 249, 126079. [PubMed: 32062554]

(71). Zhang S; Li X; Gong W; Sun T; Wang Z; Ning G Pillar[5]Arene-Derived Microporous Polyaminal Networks with Enhanced Uptake Performance for CO 2 and Iodine. Ind. Eng. Chem. Res 2020, 59 (7), 3269–3278.

(72). Yu X; Wu W; Zhou D; Su D; Zhong Z; Yang C Bisindole [3]Arenes—Indolyl Macrocyclic Arenes Having Significant Iodine Capture Capacity. CCS Chem. 2022, 4 (5), 1806–1814.

(73). Li X; Peng Y; Jia Q Construction of Hypercrosslinked Polymers with Dual Nitrogen-Enriched Building Blocks for Efficient Iodine Capture. Sep. Purif. Technol 2020, 236, 116260.

(74). Nandanwar SU; Coldsnow K; Green M; Utgikar V; Sabharwall P; Aston DE Activity of Nanostructured C@ ETS-10 Sorbent for Capture of Volatile Radioactive Iodine from Gas Stream. Chem. Eng. J 2016, 287, 593–601.

(75). Velichkina N; Vlasova T; Kalashnikov A; Kol'tsov VY Extraction of Iodine from Mother Liquors Formed as Industrial Waste with Activated Carbons. Russ. J. Appl. Chem 2014, 87 (7), 994–997.

(76). Yilmaz D; Gürol A Efficient Removal of Iodine-131 from Radioactive Waste by Nanomaterials. Instrum. Sci. Technol 2021, 49 (1), 45–54.

(77). Alsalbokh M; Fakeri N; Lawson S; Rownaghi AA; Rezaei F Adsorption of Iodine from Aqueous Solutions by Aminosilane-Grafted. Chem. Eng. J 2021, 415, 128968.

(78). Alsalbokh M; Fakeri N; Rownaghi AA; Ludlow DL; Rezaei F Aminosilane-Grafted Bismuth-Alumina Adsorbents: Role of Amine Loading and Bismuth Content in Iodine Immobilization from Aqueous Solutions. Chem. Eng. J 2021, 409, 128277.

(79). Yang JHY; Shin JM; Park JJ; Park GI; Yim MS Novel Synthesis of Bismuth-Based Adsorbents for the Removal of 129I in off-Gas. J. Nucl. Mater 2015, 457, 1–8.

(80). Yang JH; Cho Y-J; Shin JM; Yim M-S Bismuth-Embedded SBA-15 Mesoporous Silica for Radioactive Iodine Capture and Stable Storage. J. Nucl. Mater 2015, 465, 556–564.

(81). Al-Mamoori A; Alsalbokh M; Lawson S; Rownaghi AA; Rezaei F Development of Bismuth-Mordenite Adsorbents for Iodine Capture from off-Gas Streams. Chem. Eng. J 2020, 391, 123583.

(82). Huang H; Sha X; Cui Y; Sun S; Huang H; He Z; Liu M; Zhou N; Zhang X; Wei Y Highly Efficient Removal of Iodine Ions Using MXene-PDA-Ag_2Ox Composites Synthesized by Mussel-Inspired Chemistry. J. Colloid Interface Sci 2020, 567, 190–201. [PubMed: 32058169]

(83). Sha X; Huang H; Sun S; Huang H; Huang Q; He Z; Liu M; Zhou M; Zhang X; Wei Y Mussel-Inspired Preparation of MXene-PDA-Bi_6O_7 Composites for Efficient Adsorptive Removal of Iodide Ions. J. Environ. Chem. Eng 2020, 8, 104261.

(84). Sun S; Sha XS; Liang J; Yang G; Hu X; Wen Y; Liu M; Zhou N; Zhang X; Wei Y Construction of Ionic Liquid Functionalized MXene with Extremely High Adsorption Capacity towards Iodine via the Combination of Mussel-Inspired Chemistry and Michael Addition Reaction. J. Colloid Interface Sci 2021, 601 , 294–304. [PubMed: 34082233]

(85). Sun S; Sha X; Liang J; Yang G; Hu X; He Z; Liu M; Zhou N; Zhang X; Wei Y Rapid Synthesis of Polyimidazole Functionalized MXene via Microwave-Irradiation Assisted Multi-Component Reaction and Its Iodine Adsorption Performance. J. Hazard. Mater 2021, 420, 126580. [PubMed: 34252673]

(86). Hakimi Sakuma S; Marzukee N Removal of Iodine-125 from Effluents by Chemical and Soil Column Methods. J. Radioanal. Nucl. Chem 1995, 196 (1), 77–87.

(87). Decamp C; Happel S Utilization of a Mixed-Bed Column for the Removal of Iodine from Radioactive Process Waste Solutions. J. Radioanal. Nucl. Chem 2013, 298 (2), 763–767.

(88). Nandanwar SU; Coldsnow K; Porter A; Sabharwall P; Aston DE; McIlroy DN; Utgikar V Adsorption of Radioactive Iodine and Krypton from Off-Gas Stream Using Continuous Flow Adsorption Column. Chem. Eng. J 2017, 320, 222–231.

(89). Madrakian T; Afkhami A; Zolfigol MA; Ahmadi M; Koukabi N Application of Modified Silica Coated Magnetite Nanoparticles for Removal of Iodine from Water Samples. Nano-Micro Lett. 2012, 4 (1), 57–63.

(90). Attallah MF; Rizk SE; El Afifi EM Efficient Removal of Iodine and Chromium as Anionic Species from Radioactive Liquid Waste Using Prepared Iron Oxide Nanofibers. J. Radioanal. Nucl. Chem 2018, 317, 933–945.

(91). He T; Li Q; Lin T; Li J; Bai S; An S; Kong X; Song Y-F Recent Progress on Highly Efficient Removal of Heavy Metals by Layered Double Hydroxides. Chem. Eng. J 2023, 462, 142041.

(92). Fetter G; Ramos E; Olguin MT; Bosch P; Lopez T; Bulbulian S Sorption of 131I- by Hydrotalcites. J. Radioanal. Nucl. Chem 1997, 221, 63–66.

(93). Curtius H; Kattilparampil Z Sorption of Iodine on Mg-Al-Layered Double Hydroxide. Clay Miner. 2005, 40, 455–461.

(94). Weiss A; Toth E Untersuchungen Zur Synthese, Quellungseigenschaften Und Anionenaustausch von Kristallchemisch Modifizierten Doppelhydroxiden Vom Hydrotalkit-Typ (Investigations of Synthesis, Swelling Properties and Anion Exchange of Crystallochemical Modified Double Hydroxides of the Hydrotalcite Type). Contrib. Annu. DTTG Meet. Freib. Ger. Wolf R Starke R Kleeberg Ed 1996, 267–276.

(95). Kentjono L; Liu JC; Chang WC; Irawan CI Removal of Boron and Iodine from Optoelectronic Wastewater Using Mg-Al (NO_3) Layered Double Hydroxide. Desalination 2010, 262, 280–283.

(96). Theiss FL; Sear-Hall MJ; Palmer SJ; Frost RL Zinc Aluminum Layered Double Hydroxides for the Removal of Iodine and Iodide from Aqueous Solutions. Desalination Water Treat. 2012, 39 (1–3), 166–175.

(97). Yu X; Cui W; Zhang F; Guo Y; Deng T Removal of Iodine from the Salt Water Used for Caustic Soda Production by Ion-Exchange Resin Adsorption. Desalination 2019, 458, 76–83.

(98). Chen Y; Yan C; Zhao W; Liu Z; Mu T The Dynamic Process of Radioactive Iodine Removal by Ionic Liquid 1-Butyl-3-Methyl-Imidazolium Acetate: Discriminating and Quantifying Halogen Bonds versus Induced Force. RSC Adv. 2014, 4 (98), 55417–55429.

(99). Yan C; Mu T Investigation of Ionic Liquids for Efficient Removal and Reliable Storage of Radioactive Iodine: A Halogen-Bonding Case. Phys. Chem. Chem. Phys 2014, 16 (11), 5071–5075. [PubMed: 24492960]

(100). DeSilva LA; Harwell J; Gaquere-Parker A; Perera UAG; Tennakone K Thin Films of Copper (I) Iodide Doped with Iodine and Thiocyanate. Phys. Status Solidi A 2017, 214 (12), 1700520.

(101). Ali M; Changqi Y; Zhongning S; Haifeng G; Junlong W; Mehboob K Iodine Removal Efficiency in Non-Submerged and Submerged Self-Priming Venturi Scrubber. Nucl. Eng. Technol 2013, 45 (2), 203–210.

(102). Gulhane NP; Landge AD; Shukla DS; Kale SS Experimental Study of Iodine Removal Efficiency in Self-Priming Venturi Scrubber. Ann. Nucl. Energy 2015, 78, 152–159.

(103). Zhou Y; Sun Z; Gu H; Miao Z Performance of Iodide Vapours Absorption in the Venturi Scrubber Working in Self-Priming Mode. Ann. Nucl. Energy 2016, 87, 426–434.

(104). Bal M; Reddy TT; Meikap BC Performance Evaluation of Venturi Scrubber for the Removal of Iodine in Filtered Containment Venting System. Chem. Eng. Res. Des 2018, 138, 158– 167.

(105). Rosenberg BL; Steinhauser G Preparedness for a Nuclear Accident: Removal of Radioiodine from Soil by Chemical Processing. J. Radioanal. Nucl. Chem 2016, 307, 1765–1769.

(106). Mu WJ; Yu QH; Li XL; Wei HY; Jian Y Niobate Nanofibers for Simultaneous Adsorptive Removal of Radioactive Strontium and Iodine from Aqueous Solution. J. Alloys Compd 2017, 693, 550–555.

(107). Yang OB; Kim JC; Lee JS; Kim YG Use of Activated Carbon Fiber for Direct Removal of Iodine from Acetic Acid Solution. Ind. Eng. Chem. Res 1993, 32 (8), 1692–1697.

(108). Rong J; Zhao Z; Jing Z; Zhang T; Qiu F; Xu J High-Specific Surface Area Hierarchical Al_2O_3 Carbon Fiber Based on A Waste Paper Fiber Template: Preparation and Adsorption for Iodide Ions. J. Wood Chem. Technol 2017, 37 (6), 485–492.

(109). Qian Q; Shao S; Yan F; Yuan G Direct Removal of Trace Ionic Iodide from Acetic Acid via Porous Carbon Spheres. J. Colloid Interface Sci 2008, 328 (2), 257–262. [PubMed: 18922541]

(110). Ikari M; Matsui Y; Suzuki Y; Matsushita T; Shirasaki N Removal of Iodide from Water by Chlorination and Subsequent Adsorption on Powdered Activated Carbon. Water Res. 2015, 68, 227–237. [PubMed: 25462731]

(111). Sun L; Li K; Huang J; Jiang Z; Huang Y; Liu H; Wei G; Ge F; Ye X; Zhang Y; et al. Facile Synthesis of Tri (Octyl-Decyl) Amine-Modified Biomass Carbonaceous Aerogel for Rapid Adsorption and Removal of Iodine Ions. Chem. Eng. Res. Des 2019, 144, 228–236.

(112). Sun L; Zhang Y; Ye X; Liu H; Zhang H; Wu A; Wu Z Removal of I–from Aqueous Solutions Using a Biomass Carbonaceous Aerogel Modified with KH-560. ACS Sustain. Chem. Eng 2017, 5 (9), 7700–7708.

(113). Mushtaq S; Yun S-J; Yang JE; Jeong S-W; Shim HE; Choi MH; Park SH; Choi YJ; Jeon J Efficient and Selective Removal of Radioactive Iodine Anions Using Engineered Nanocomposite Membranes. Environ. Sci. Nano 2017, 4, 2157–2163.

(114). Sánchez-Polo M; Rivera-Utrilla J; Salhi E; von Gunten U Removal of Bromide and Iodide Anions from Drinking Water by Silver-Activated Carbon Aerogels. J. Colloid Interface Sci 2006, 300 (1), 437–441. [PubMed: 16696995]

(115). Yu F; Chen Y; Wang Y; Liu C; Ma W Enhanced Removal of Iodide from Aqueous Solution by Ozonation and Subsequent Adsorption on Ag-Ag_2O Modified on Carbon Spheres. Appl. Surf. Sci 2018, 427, 753–762.

(116). Zhang X; Gu P; Zhou S; Li X; Zhang G; Dong L Enhanced Removal of Iodide Ions by Nano Cu_2/Cu Modified Activated Carbon from Simulated Wastewater with Improved Countercurrent Two-Stage Adsorption. Sci. Total Environ 2018, 626, 612–620. [PubMed: 29358140]

(117). Han S; Um W; Kim W-S Development of Bismuth-Functionalized Graphene Oxide to Remove Radioactive Iodine. Dalton Trans. 2019, 48, 478–485. [PubMed: 30520479]

(118). Nabipoor Hassankiadeh M; Moghadamrezaee M; Golmohammadi M; Naderifar A Ag/ Amberlyst 15: Novel Adsorbent for Removal of Iodide Compounds From the Acetic Acid Solution. Chem. Eng. Commun 2015, 202 (8), 993–999.

(119). Ye Z; Chen L; Liu C; Ning S; Wang X; Wei Y The Rapid Removal of Iodide from Aqueous Solutions Using a Silica-Based Ion-Exchange Resin. React. Funct. Polym 2019, 135, 52–57.

(120). Sarri S; Misaelides P; Noli F; Papadopoulou L; Zamboulis D Removal of Iodide from Aqueous Solutions by Polyethylenimine-Epichlorohydrin Resins. J. Radioanal. Nucl. Chem 2013, 298 (1), 399–403.

(121). Baimenov A. Zh; Berillo DA; Inglezakis VJ Cryogel-Based Ag°/Ag_2O Nanocomposites for Iodide Removal from Water. J. Mol. Liq 2020, 299, 112134.

(122). Zia MR; Raza MA; Park SH; Irfan N; Ahmed R; Park JE; Jeon J; Mushtaq S Removal of Radioactive Iodine Using Silver/Iron Oxide Composite Nanoadsorbents. Nanomaterials 2021, 11 (3), 588. [PubMed: 33652803]

(123). Mao P; Liu Y; Liu X; Wang Y; Liang J; Zhou Q; Dai Y; Jiao Y; Chen S; Yang Y Bimetallic AgCu/Cu_2O Hybrid for the Synergetic Adsorption of Iodide from Solution. Chemosphere 2017, 180, 317–325. [PubMed: 28412489]

(124). Mao P; Qi L; Liu X; Liu Y; Jiao Y; Chen S; Yang Y Synthesis of Cu/Cu_2O Hydrides for Enhanced Removal of Iodide from Water. J. Hazard. Mater 2017, 328, 21–28. [PubMed: 28076769]

(125). Jang J; Lee DS Magnetite Nanoparticles Supported on Organically Modified Montmorillonite for Adsorptive Removal of Iodide from Aqueous Solution: Optimization Using Response Surface Methodology. Sci. Total Environ 2018, 615, 549–557. [PubMed: 28988090]

(126). Tauanov Z; Inglezakis VJ Removal of Iodide from Water Using Silver Nanoparticles-Impregnated Synthetic Zeolites. Sci. Total Environ 2019, 682, 259–270. [PubMed: 31125740]

(127). Inglezakis VJ; Satayeva A; Yagofarova A; Tauanov Z; Meiramkulova K; Farrando-Pérez J; Bear JC Surface Interactions and Mechanisms Study on the Removal of Iodide from Water by Use of Natural Zeolite-Based Silver Nanocomposites. Nanomaterials 2020, 10 (6), 1156. [PubMed: 32545557]

(128). Zhao X; Han X; Li Z; Huang H; Liu D; Zhong C Enhanced Removal of Iodide from Water Induced by a Metal-Incorporated Porous Metal–Organic Framework. Appl. Surf. Sci 2015, 351, 760–764.

(129). Zhang T; Yue X; Gao L; Qiu F; Xu J; Rong J; Pan J Hierarchically Porous Bismuth Oxide/Layered Double Hydroxide Composites: Preparation, Characterization and Iodine Adsorption. J. Clean. Prod 2017, 144, 220–227.

(130). Liang L; Li L Adsorption Behavior of Calcined Layered Double Hydroxides towards Removal of Iodide Contaminants. J. Radioanal. Nucl. Chem 2007, 273 (1), 221–226.

(131). Ma S; Islam SM; Shim Y; Gu Q; Wang P; Li H; Sun G; Yang X; Kanatzidis MG Highly Efficient Iodine Capture by Layered Double Hydroxides Intercalated with Polysulfides. Chem. Mater 2014, 26 (24), 7114–7123.

(132). Jung I-K; Jo Y; Han S-C; Yun J-I Efficient Removal of Iodide Anion from Aqueous Solution with Recyclable Core-Shell Magnetic Fe_3O_4@Mg/Al Layered Double Hydroxide (LDH). Sci. Total Environ 2020, 705, 135814. [PubMed: 31972945]

(133). Theiss FL; Sear-Hall MJ; Palmer SJ; Frost RL Zinc Aluminium Layered Double Hydroxides for the Removal of Iodine and Iodide from Aqueous Solutions. Desalination Water Treat. 2012, 39 (1–3), 166–175.

(134). Zhang L; Jaroniec M SBA-15 Templating Synthesis of Mesoporous Bismuth Oxide for Selective Removal of Iodide. J. Colloid Interface Sci 2017, 501, 248–255. [PubMed: 28458225]

(135). Sha X; Huang H; Sun S; Huang H; Huang Q; He Z; Liu M; Zhou N; Zhang X; Wei Y Mussel-Inspired Preparation of Mxene-Pda-Bi_6O_7 Composites for Efficient Adsorptive Removal of Iodide Ions. J. Environ. Chem. Eng 2020, 8 (5), 104261.

(136). Liu Y; Gu P; Jia L; Zhang G An Investigation into the Use of Cuprous Chloride for the Removal of Radioactive Iodide from Aqueous Solutions. J. Hazard. Mater 2016, 302, 82–89. [PubMed: 26448493]

Selected Iodine-Containing Organic Compounds

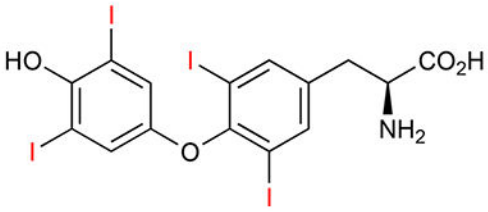

L-Thyroxine

Tyrosine-based hormone

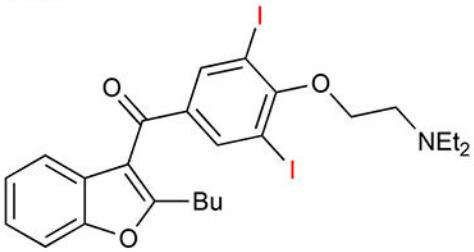

Amiodarone

Antiarrhythmic drug

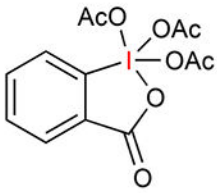

Dess-Martin periodinane

Chemical reagent: Oxidant

Selected Iodine-Containing Inorganic Compounds

Compound Name	Formula	Applications
Ammonium iodide	(NH_4I):	*Photograhy, synthesis, and some medications.*
Copper iodide	(CuI):	*Synthesis and catalysis.*
Hydroiodic acid	(HI):	*Synthesis: In preparation of alkyl iodides.*
Iodine	(I_2):	*Medicine and chemistry.*
Lead(II) iodide	(PbI_2):	*Pigments, solar cells, and photon detectors.*
Lithium iodide	(LiI):	*Synthesis, radiocontrast agent for CT scans, and as electrolyte.*
Potassium iodate	(KIO_3):	*Iodized salt and as oxidizing agent.*
Potassium iodide	(KI):	*Iodized salt, for radiation protection, and as oxidizing agent.*
Silver iodide	(AgI):	*Photography, as antiseptic, and in cloud seeding.*
Sodium iodate	($NaIO_3$):	*Iodized salt and as oxidizing agent.*
Sodium iodide	(NaI):	*Organic chemistry, as a nutritional supplement, and nuclear medicine.*
Tungsten iodide	(WI_3):	*Stabilize filaments in light bulbs.*

Figure 1.

Notable iodine containing compounds and their applications.

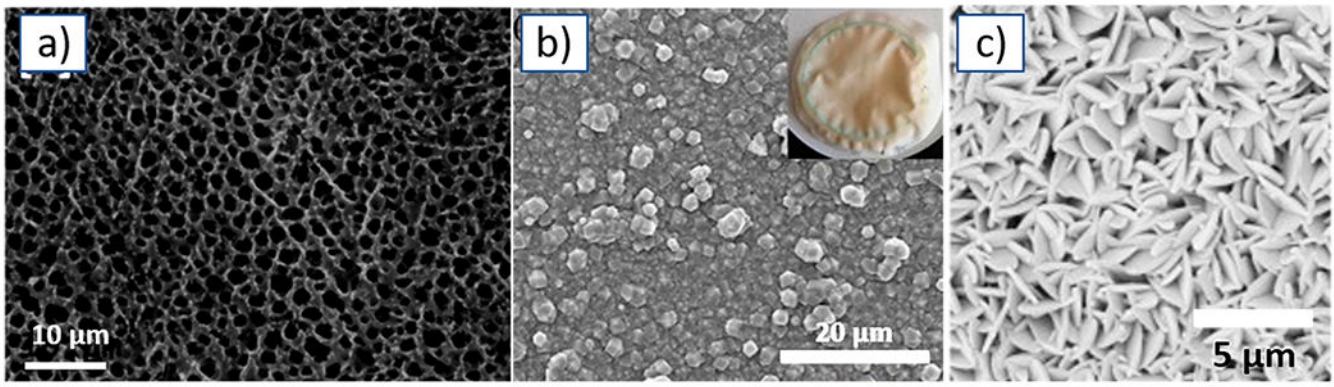

Figure 2.

SEM images of (a) cross-linked chitosan MOF, (b) PVDF/ZIF-8 nanocomposite, and (c) ZIF-L@SiC. Reprinted with permission from refs 52, 53, and 54. Copyright 2020 Elsevier, 2020 Elsevier, and 2021 Elsevier, respectively.

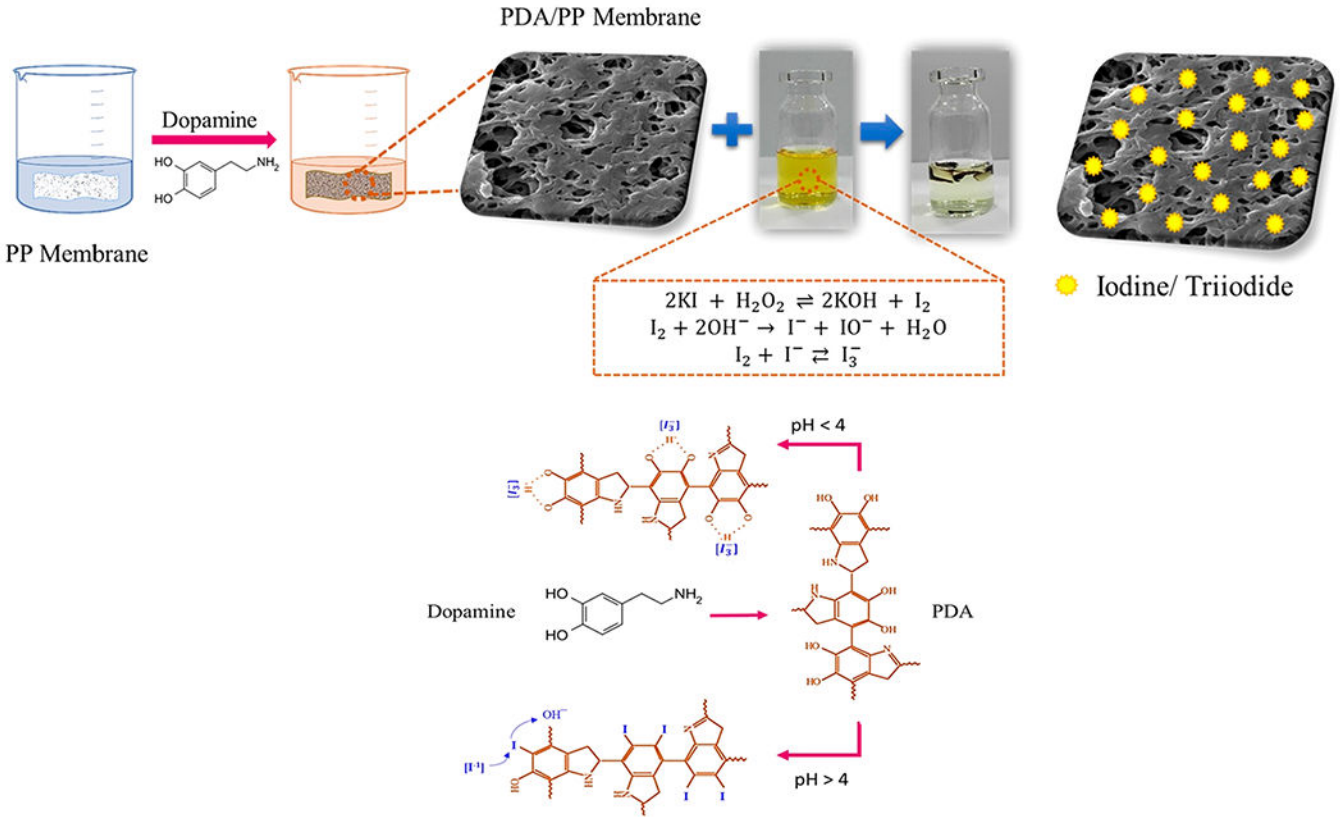

Figure 3.

Scheme depicting the mechanism of iodine removal via the polypropylene/polydopamine membrane. Reprinted with permission from ref 70. Copyright 2020 Elsevier.

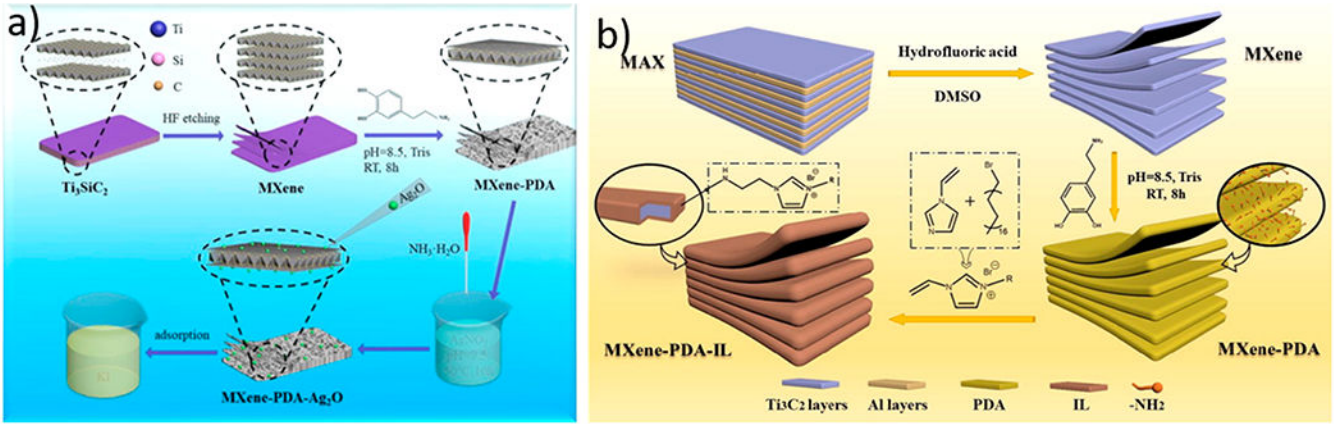

Figure 4.

(a) Scheme illustrating surface modification of delaminated MXene with silver oxide. Reprinted with permission from ref 82. Copyright 2020 Elsevier. (b) Scheme representing preparation of MXene-PDA-IL from MXene through the combination of mussel-inspired chemistry and Michael addition reaction. Reprinted with permission from ref 84. Copyright 2021 Elsevier.

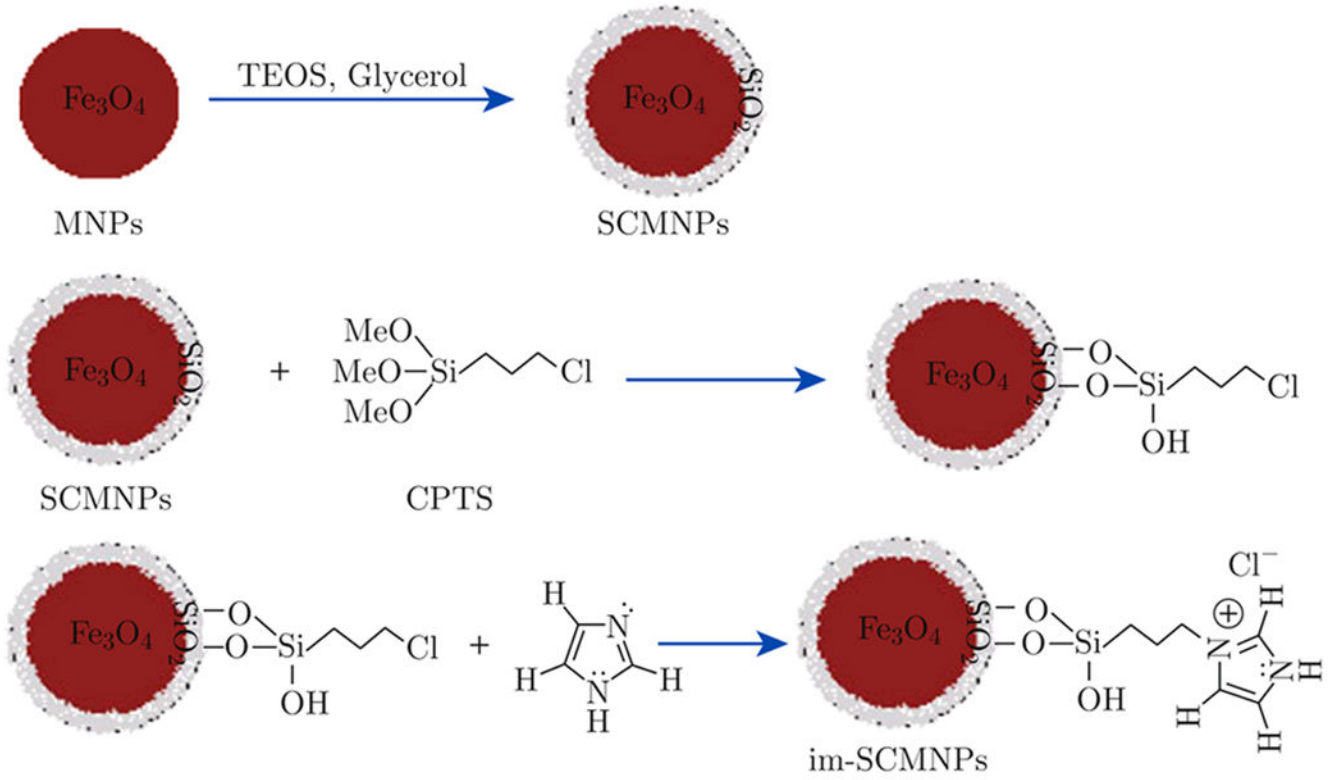

Figure 5.

Reaction scheme illustrating the modification of magnetic nanoparticles with imidazole (im-SCMNPs). Reprinted with permission from Madrakian, T.; Afkhami, A.; Zolfigol, M. A.; Ahmadi, M.; Koukabi, N. *Nano-Micro Lett.* **2012**, *4*, 57–63. Copyright 2012 Springer. Licensed under CC-BY-4.0, https://creativecommons.org/licenses/by/4.0/.

Figure 6.
Purification system used in this work for the removal of iodine from salt water: (a) adsorption system and (b) control system. Reprinted with permission from ref 97. Copyright 2019 Elsevier.

Figure 7.
Picture of the experimental setup of a venturi scrubber using a filtered containment venting system. Reprinted with permission from ref 104. Copyright 2018 Elsevier.

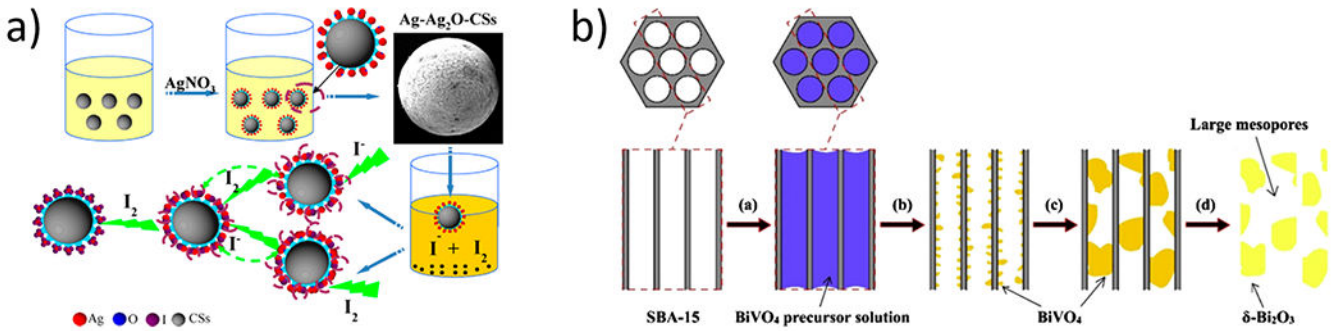

Figure 8.

Scheme depicting the synthesis of materials used for iodide extraction: (a) Ag-Ag_2O-coated carbon sphere composite material and (b) Bi_2O_3-decorated mesoporous silica. Reprinted with permission from refs 115 and 134. Copyright 2018 Elsevier and 2017 Elsevier, respectively.

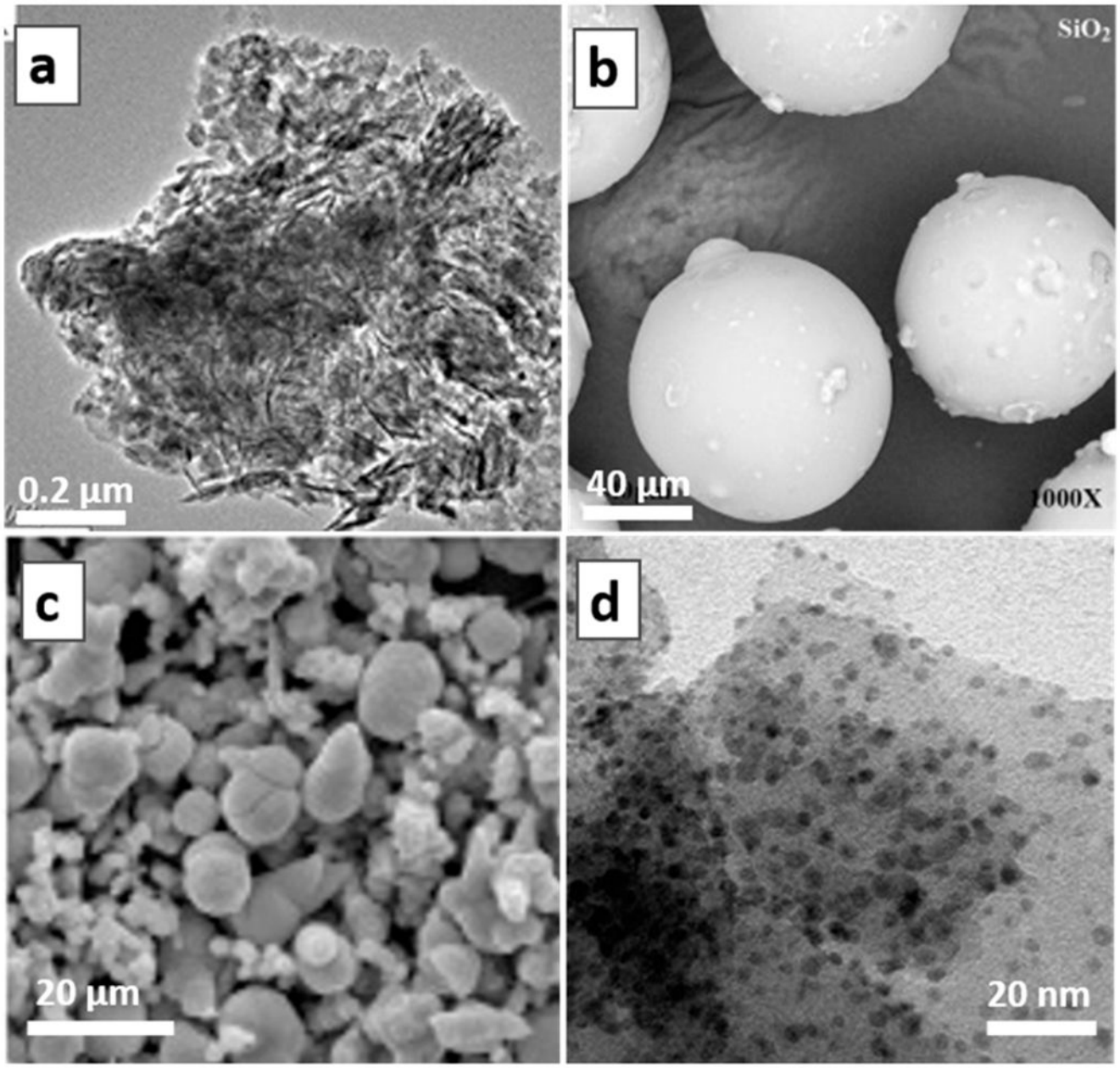

Figure 9.

(a) Hierarchical Al_2O_3 carbon fiber, (b) silica-based polymeric ion-exchange resin, (c) bimetallic AgCu/Cu_2O nanoparticles, and (d) Ag-zeolite nanocomposite. Reproduced with permission from refs 108, 119, and 124. Copyright 2017 Elsevier, 2019 Elsevier, and 2017 Elsevier, respectively. Reprinted with permission from Inglezakis, V. J.; Satayeva, A.; Yagofarova, A.; Tauanov, Z.; Meiramkulova, K.; Farrando-Pérez, J.; Bear, J. C. *Nanomaterials* **2020**, *10*, 1156. Copyright 2020 Multidisciplinary Digital Publishing Institute. Licensed under CC-BY-4.0, https://creativecommons.org/licenses/by/4.0/.

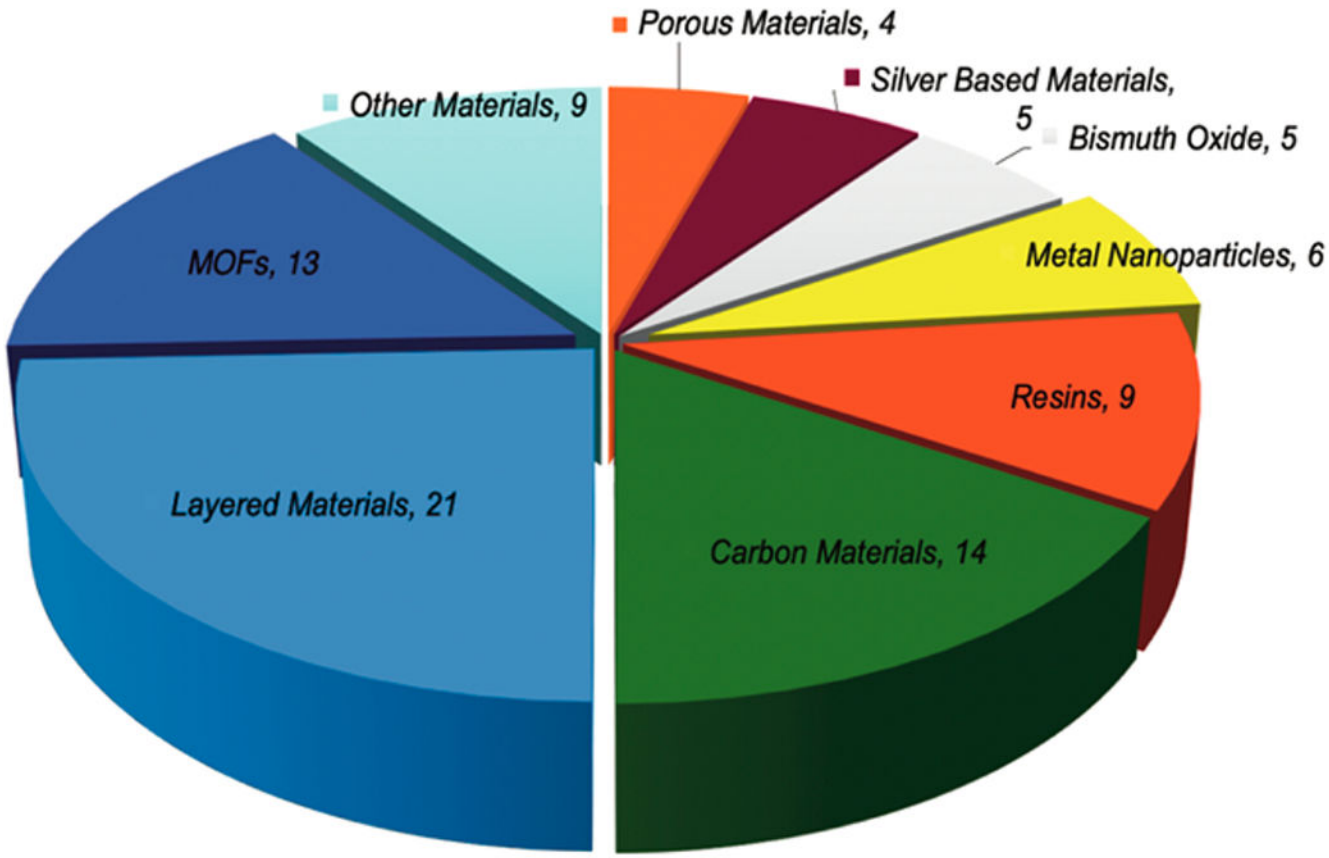

Figure 10.
Different categories of adsorbents with the number of appearances (articles) given in this Review.

Table 1.

Iodine Adsorption Capacities and Removal Efficiencies of Various Materials

Material	Adsorption capacity (mg/g)	Removal efficiency (%)	Ref
$\{[Zn_3(DL\text{-}lac)_2(pybz)_2]\cdot 2.5DMF\}_n$ (lac-Zn)	755	92.98	51
Epichloridine-2-aminoterephthalic acid-chitosan	399.68	–	52
PVDF/ZIF-8	73.33	73	53
ZIF-L	–	100	54
Cu_2O/TMU-17-NH_2	567	–	55
Zirconium-based MOFs	1.42	–	56
Zeolitic imidazolate loaded in porous natural basswood	1.09	–	57
$\{[Mn_2(oxdz)_2(tpbn)(H_2O)_2]\cdot 2C_2H_5OH\}$ n, with a heterocyclic dicarboxylate linker (H_2oxdz:(4,4′-(1,3,4-oxadiazole-2,5-diyl)dibenzoic acid))	1.1	100	58
COF-DL229	2300	66	60
Tfp-COFs	5820	99.9	61
$Ni_3(BTC)_2\cdot 12H_2O$ (NiBTC)	160	–	63
AgAero	88	–	65
$Pb_{10}(VO_4)_6I_2$	–	94.62	67
Ag-Alumina	–	99	68
DTO-BTT-THO	326	–	69
PP/PDA membrane	245	75	70
PAN-FPP5	700	70	71
2,4,6-Triphenyl-1,3,5-triazine-pyrrole	–	8.04	73
Supported hollow carbon nanostructured polyhedron adsorbent material	40		74
KAD coal	1030	–	75
Single-walled carbon nanotubes (SWNTs)	1.356	22.60	76
Graphene oxide	1.081	18.01	76
–COOH-functionalized SWNT	0.917	15.28	76
Graphene	0.878	14.63	76

Table 2.

Iodine Adsorption Capacities and Removal Efficiencies of Various Materials

Adsorbent material	Adsorption capacity (mg/g)	Removal efficiency (%)	Ref
Al-DMAPS	241	95	77
Al-APS	124	51	77
Al-MAPS	223	87	77
Bi_{15}/Al-DMAPS	251.5	–	78
PVA	468	–	79
Bi-SBA-15-SH	540	–	80
Bi_5@modernite	538	–	81
MXene-PDA-Ag_2Ox	80	80	82
MXene-PDA-Bi_6O_7	64.65	–	83
MXene-PDA-IL	694.4	90	84
MXene-PIL	170	–	85
Mixed-bed column	–	88 ± 5	87
C@ETS-10	57.77	–	88
im-SCMNPs	140.84	98	89
SH1 nanofibers	26.74	90	90
Mg-Al-Cl-LDH	500	–	93
Mg-Al (NO_3) LDH	10.1	–	95
Zn/Al LDH	–	99.5 (I_2), 36.8 (I^-)	96
Ionic liquids	80	98–99	99
Submerged self-priming venturi scrubber	–	99.9 ± 0.1	101
Self-priming venturi scrubber	–	66.62	102
Self-priming venturi scrubber	–	99	103
Venturi scrubber	–	82.32	104
Soil treated with $AgNO_3$	–	45 ± 1	105
Soil treated with H_2O_2 and HNO_3	–	17 ± 1	105
Ag_2O-SNF	296	97	106

Table 3.

Iodide Adsorption Capacities and Removal Efficiencies of Various Materials

Material	Adsorption capacity (mg/g)	Removal efficiency (%)	Ref
Activated carbon fiber	350	90	107
Al_2O_3 activated carbon	–	92.3	108
Poly(vinylidene) chloride carbon sphere	–	70	109
Activated carbon	–	90	110
Carbon aerogel chemically modified with tri(octyl-decyl) amine	107.9	–	111
(3-Glycidyloxypropyl) trimethoxysilane carbon-based aerogel	317	–	112
Au-CAM membrane	–	99.88	113
Ag-carbon aerogels	–	–	114
Ag-Ag_2O carbon sphere	374. 91	–	115
Cu_2O/Cu carbon sphere	–	90	116
Bi-GO	230	≥95	117
Ag/Amberlyst 15	–	99 (CH_3I)	118
Si-poly(4-vinylpyridine)	149	96	119
polyethylenimine-epichlorohydrin	649	–	120
Ag°/Ag_2O cryogels	326	–	121
Ag/Fe_3O_4	847	–	122
AgCu/Cu_2O	65.2	85.1	123
Cu/Cu_2O	25	–	124
Magnetic NPs-montmorillonite	322.42	93.81	125
Ag-NP zeolite	20.44	94.85	126
Ag-natural zeolite	132	95	127
Ag-MOF	242	–	128
$Bi_2O_{2.33}$	284.9	–	48
Bi_2O_3/LDH	101.9	94	129
Mg/Al-CLDH	376	–	130
Fe_3O_4@Mg/Al-LDH	105	80	132
Zn/Al-LDH	–	36.8	133
SBA-15-Bi_2O_3	364	91	134
MXene-PDS-Bi_6O_7	64.65	–	135
CuCl	–	95.8	136